

Beyond Single: A Data Selection Principle for LLM Alignment via Fine-Grained Preference Signals

Jia Zhang^{1,2}, Yao Liu³, Chen-Xi Zhang^{1,2}, Yi Liu³, Yi-Xuan Jin³,
 Lan-Zhe Guo^{1,4,†}, Yu-Feng Li^{1,2,†}

¹ National Key Laboratory for Novel Software Technology, Nanjing University

² School of Artificial Intelligence, Nanjing University

³ Algorithm Tech, Taobao & Tmall Group of Alibaba

⁴ School of Intelligence Science and Technology, Nanjing University

† Corresponding Author

Abstract

Aligning Large Language Models (LLMs) with diverse human values requires moving beyond a single holistic “better-than” preference criterion. While collecting fine-grained, aspect-specific preference data is more reliable and scalable, existing methods like Direct Preference Optimization (DPO) struggle with the severe noise and conflicts inherent in such aggregated datasets. In this paper, we tackle this challenge from a data-centric perspective. We first derive the Direct Multi-Preference Optimization (DMPO) objective, and uncover a key Preference Divergence (PD) term that quantifies inter-aspect preference conflicts. Instead of using this term for direct optimization, we leverage it to formulate a novel, theoretically-grounded data selection principle. Our principle advocates for selecting a subset of high-consensus data—identified by the most negative PD values—for efficient DPO training. We prove the optimality of this strategy by analyzing the loss bounds of the DMPO objective in the selection problem. To operationalize our approach, we introduce practical methods of PD term estimation and length bias mitigation, thereby proposing our PD selection method. Evaluation on the UltraFeedback dataset with three varying conflict levels shows that our simple yet effective strategy achieves over 10% relative improvement against both the standard holistic preference and a stronger oracle using aggregated preference signals, all while boosting training efficiency and obviating the need for intractable holistic preference annotating, unlocking the potential of robust LLM alignment via fine-grained preference signals.

1 Introduction

Reinforcement Learning from Human Feedback (RLHF) (Christiano et al. 2017; Ouyang et al. 2022; Bai et al. 2022) plays a pivotal role in aligning Large Language Models (LLMs) (Naveed et al. 2024; Brown et al. 2020; Meta AI 2023). However, standard RLHF methods of online reinforcement learning (Schulman et al. 2017; Shao et al. 2024) are often plagued by substantial computational overhead and the complex, multi-stage training process. As an efficient alternative, Direct Preference Optimization (DPO) (Rafailov et al. 2023) directly aligns LLMs by fine-tuning them on an offline dataset of human preferences, bypassing the need for the complex and unstable RL-based methods.

Preprint. Under review

The efficacy of DPO is tied to the quality of the offline preference dataset. Typically, practitioners collect and annotate data by soliciting judgments from *human annotators* or stronger *teacher models* (Ziegler et al. 2020; Stiennon et al. 2020; Bai et al. 2022) to label a *winner* from two responses for a given prompt. However, this paradigm rests on the implicit but often untenable assumption that a single, holistic, and tractable criterion for preference annotating exists. In many cases, it is often ambiguous which of two candidates is definitively superior under a holistic criterion (Bakker et al. 2022; Casper et al. 2023). Specifically, the ambiguity stems from two primary issues. 1) Defining a single, comprehensive criterion is inherently challenging, causing annotators with diverse biases to struggle with a consistent judgment. 2) Responses often exhibit quality trade-offs, where one is rarely superior across all aspects. This complexity makes it intractable for annotators to provide reliable judgments and annotations. Consequently, the resulting inconsistent and unreliable preference signals risk undermining the effectiveness of alignment methods.

Instead of relying on a holistic, ambiguous “better-than” judgment, some studies (Ji et al. 2023; Wu et al. 2023; Rame et al. 2023) argue that the preference can be decomposed into multiple, fine-grained aspects, which we term *sub-preferences* for simplicity. For example, judging if a response is superior in terms of logical consistency, factual accuracy, or instructional clarity is more tractable than making a holistic quality assessment. Such fine-grained criteria are much easier to define precisely, facilitating annotators to provide more reliable and consistent preference labels, as annotators can then focus on one clear aspect at a time.

Leveraging aggregated datasets sourced from various sub-preference criteria appears promising for alignment, given their ease of acquisition and higher reliability. However, this path faces two hurdles. 1) Existing DPO-style methods are mainly designed for a single preference criterion and lack mechanisms to handle multiple fine-grained preference signals. 2) More critically, aggregating data from diverse sub-preferences introduces severe data quality issues, such as redundancy, noise, and preference conflicts, leading to training inefficiency and performance degradation. For instance, the statistical analysis in Figure 1 of the widely-used preference dataset UltraFeedback (Cui et al. 2023), which provides an-

notations of fine-grained aspects, reveals that nearly 30% of samples exhibit explicit conflict between fine-grained and holistic preferences. This predicament raises a critical research question: How can we effectively harness these aggregated datasets with fine-grained preference signals for robust model alignment, especially in the presence of inherent and severe preference conflicts and noise?

In this paper, we explore the understudied alignment scenario of using fine-grained preference data and signals from a data-centric perspective. We begin by deriving the objective for Direct Multi-Preference Optimization (DMPO) that utilizes all signals for alignment. Inspired by the insight that the DMPO assigns varying importance to preference data, we formulate a theoretically-grounded data selection principle based on preference divergence by proving the optimal loss bounds of DMPO in the selection problem. To facilitate the usability in practice, we propose PD term estimation and length bias mitigation, resulting in our final simple but effective data selection algorithm for LLM alignment.

We evaluated our method on the UltraFeedback dataset under various preference conflict scenarios. Leveraging only fine-grained preference signals, our approach consistently outperforms baselines trained on both holistic and even stronger oracle preference, while simultaneously boosting training efficiency and obviating the need for intractable holistic preference annotating. This demonstrates the effectiveness of our strategy in filtering high-quality data from datasets with noise and conflicts, enabling more robust and efficient alignment using fine-grained preference signals.

To summarize, our contributions are as follows:

- (1) **Selection Problem:** To address data issues such as noises and conflicts in alignment using fine-grained preference signals, we formalize the data selection problem grounded in insights from the derived DMPO objective.
- (2) **Principled Method:** We propose a novel, theoretically-grounded data selection principle: train only on a subset of high-consensus data identified by the most negative PD values. To operationalize this, we introduce practical methods of PD term estimation and length bias mitigation, resulting in our PD selection method.
- (3) **Empirical Validation:** Extensive experiments show that our selection method outperforms the standard holistic preference and a stronger oracle baseline across varying conflict levels, demonstrating its effectiveness in filtering for high-quality data from datasets with fine-grained preference signals for LLM alignment.

2 Related Work

2.1 Preference Alignment

Preference alignment is crucial for ensuring that the behavior of LLMs conforms to the expectations of human values. Prominent alignment methods include supervised fine-tuning (SFT) (Wei et al. 2022; Ouyang et al. 2022), reinforcement learning fine-tuning (RLFT) (Schulman et al. 2017; Shao et al. 2024; Hu et al. 2025), and DPO-style approaches (Rafailov et al. 2023; Azar et al. 2024; Ethayarajh et al. 2024; Meng, Xia, and Chen 2024) which directly optimize the model on preference pairs. While the majority of

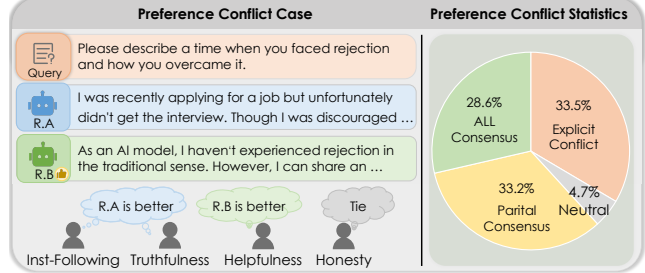


Figure 1: Conflicts between the fine-grained and holistic preferences commonly occur, and only a part of the samples show complete consistency across all fine-grained aspects.

existing work concentrates on aligning LLMs to a single “better-than” preference, a few studies (Ji et al. 2023; Wu et al. 2023; Rame et al. 2023; Zhou et al. 2024) have made preliminary attempts at multi-preference alignment, aiming to achieve Pareto-optimal by applying different weights to various preferences. In contrast, our work pioneers a data-centric perspective to tackle the severe data quality issues inherent in aggregated fine-grained preference datasets.

2.2 Data Selection and Filtering for LLM

Data selection and filtering are widely recognized as critical factors in both the pre-training and post-training stages of LLMs. For pre-training, studies (Xie et al. 2023; Gu et al. 2025; Wang et al. 2025) focus on filtering for higher-quality subsets to enhance model capabilities. In the post-training phase, particularly for SFT, numerous works (Kung et al. 2023; Xia et al. 2024; Li et al. 2024; Zhang et al. 2025) have proposed diverse metrics and strategies to select optimal data, since harmful or redundant examples can degrade fine-tuning outcomes. Existing data selection methods for DPO and RLFT (Deng et al. 2025; Lee et al. 2025; Gao et al. 2025; Li, Zou, and Liu 2025) are primarily limited to single-preference scenarios. The core mechanism of these methods often involves using an internal or external reward model to gauge sample difficulty and perform filtering. Our study stems from a key insight derived from the DMPO objective, motivating our data selection principle for more effective LLM alignment using fine-grained preference data.

3 DMPO and Preference Divergence

We begin by formalizing settings of alignment with fine-grained preferences and deriving the DMPO objective. Analysis of this objective motivates our core proposal: the Preference Divergence (PD) selection principle. We then theoretically establish this principle by deriving the optimal loss bounds for the formalized data selection problem.

3.1 DMPO Settings

We first state the following definitions about the aggregated preference dataset that was gathered from multiple fine-grained preference aspects, or sub-preferences.

Definition 3.1. A sub-preference dataset D_k is a collection of preference data (x^k, y_w^k, y_l^k) by a specific fine-grained preference criterion k . The entire aggregated dataset $D = \{(k, x^k, y_w^k, y_l^k) \mid k \in [\kappa], (x^k, y_w^k, y_l^k) \in D_k\}$ is consisted of κ sub-preference datasets from different aspects.

Definition 3.2. Each sub-preference is assumed to be modeled by a corresponding latent reward model $r_k(x, y)$, such that $r_k(x^k, y_w^k) > r_k(x^k, y_l^k), \forall (x^k, y_w^k, y_l^k) \in D_k$.

Definition 3.3. (Preference Conflict) Assume there is a ground-truth holistic reward model r^* . A conflict between fine-grained and holistic preferences occurs for sample (x^k, y_w^k, y_l^k) , such that $r_k(x^k, y_w^k) > r_k(x^k, y_l^k)$ while $r^*(x^k, y_w^k) < r^*(x^k, y_l^k)$ for some sub-preference k .

Definition 3.4. (PPO for Multiple Sub-Preferences) Given a supervised fine-tuned model or initial policy π_{ref} , the standard PPO objective of RL fine-tuning (Schulman et al. 2017) with multiple sub-preferences can be formulated as follows,

$$\arg \max_{\pi_\theta} \mathbb{E}_{x \sim D, y \sim \pi_\theta(\cdot|x)} \left[\frac{1}{\kappa} \sum_k r_k(x, y) \right] - \beta \mathbb{E}_{x \sim D} [\mathbb{D}_{\text{KL}}(\pi_\theta(\cdot|x) \parallel \pi_{\text{ref}}(\cdot|x))] \quad (1)$$

DMPO Objective. We derive the DMPO objective by extending the principles of DPO (Rafailov et al. 2023) to the multi-preference setting, resulting in the following loss function (see appendix for a full derivation from Eq. (1)):

$$\mathcal{L}_{\text{DMPO}}(\theta) = -\mathbb{E}_{z \sim D} \left[\log \sigma \left(\kappa M_\theta(z) + \underbrace{\Delta \phi_k(z)}_{\text{PD term}} \right) \right] \quad (2)$$

Here, $M_\theta(z)$ represents the preference margin,

$$M_\theta(z) = \beta \log \frac{\pi_\theta(y_w^k|x^k)}{\pi_{\text{ref}}(y_w^k|x^k)} - \beta \log \frac{\pi_\theta(y_l^k|x^k)}{\pi_{\text{ref}}(y_l^k|x^k)} \quad (3)$$

while we introduce $\Delta \phi_k(z)$ as the preference divergence (PD) term, formally defined as:

$$\Delta \phi_k(z) = \phi_k(x^k, y_w^k) - \phi_k(x^k, y_l^k) \quad (4)$$

$$\phi_k(x, y) = - \sum_{k' \neq k} r_{k'}(x, y) \quad (5)$$

3.2 Selection Insight from PD Term

The key distinction between DPO and our DMPO is the PD term, which functions as an implicit data weighting mechanism. We analyze two opposing scenarios to provide an intuitive understanding of its role:

- $\Delta \phi_k(z) > 0$: A positive PD term indicates that the sub-preference signal of aspect k conflicts with the majority of other aspects. Forcing the model to learn from such a sample may be detrimental to overall behavior. The positive PD term in DMPO reduces the sample's impact on the loss, thereby mitigating the preference margin.
- $\Delta \phi_k(z) < 0$: A negative PD term suggests the sub-preference signal of this data aligns well with the consensus of others, potentially a high-quality, reliable sample. The negative PD term in DMPO up-weights the sample's priority, reinforcing the log-probability margin.

Our analysis reveals that the PD term implicitly re-weights samples by measuring the consensus or conflict among fine-grained preference aspects. Despite its potential, DMPO still faces practical challenges, such as high computational cost and the risk of instability from unavailable or unreliable reward models. However, given the varying value and importance of samples, a natural question arises: can we devise a strategy to pre-emptively filter the dataset? Such a strategy would aim to curate a high-quality subset that improves alignment performance while enhancing training efficiency.

3.3 PD Selection Principle

Accordingly, instead of leveraging PD terms for direct optimization, we propose to use them as the basis for data selection. The goal is to find a subset of data for standard DPO, such that the resulting policy also minimizes the DMPO objective. We formalize this selection problem and present our key theorems below, which ground the validity of our selection principle. All proofs are deferred to the appendix.

Definition 3.5. (Data Selection Problem for DMPO) Assume the ϕ_k are known. Give a dataset D consists of data from κ sub-preference dataset $D_k, k \in [\kappa]$, a supervised fine-tuned model π_{ref} , the DPO objective \mathcal{L}_{DPO} , the DMPO objective $\mathcal{L}_{\text{DMPO}}$, a selection budget $\lambda = |\tilde{D}|/|D|$. The goal is to find a selection strategy that selects for a subset $\tilde{D} \subset D$ for DPO training, which results in optimal $\mathcal{L}_{\text{DMPO}}$:

$$\begin{aligned} \tilde{D} &= \arg \min_{\tilde{D} \subset D} \mathcal{L}_{\text{DMPO}}(\pi_{\tilde{\theta}}, \tilde{D}) \\ \text{s.t. } \pi_{\tilde{\theta}} &= \arg \min_{\pi_{\theta}} \mathcal{L}_{\text{DPO}}(\pi_{\theta}, \tilde{D}) \end{aligned} \quad (6)$$

Theorem 3.6. (Loss Bounds of DMPO in Data Selection Problem) Consider the learned policy $\pi_{\tilde{\theta}}$ was only trained on the subset \tilde{D} . Assume $\pi_{\tilde{\theta}}$ gives preference margin on \tilde{D} bounded by $M_{\tilde{\theta}}(z) \in [c_1, c_2]$ and suboptimal expected and bounded preference margin and loss on $D \setminus \tilde{D}$, such that $\mathbb{E}_{D \setminus \tilde{D}} [-\log \sigma(\kappa M_{\tilde{\theta}}(z))] \leq l_1, \mathbb{E}_{D \setminus \tilde{D}} [M_{\tilde{\theta}}(z)] \leq c_0$. Then, the DMPO loss is bounded as follows,

$$\mathcal{L}_{\text{DMPO}}^{\text{lower}}(\tilde{D}) \leq \mathcal{L}_{\text{MDPO}} \leq \mathcal{L}_{\text{DMPO}}^{\text{upper}}(\tilde{D}) \quad (7)$$

$$\begin{aligned} \mathcal{L}_{\text{DMPO}}^{\text{lower}}(\tilde{D}) &= -\lambda \log \sigma(\kappa c_2 + \mathbb{E}_{\tilde{D}} [\Delta \phi_k(z)]) \\ &\quad - (1 - \lambda) \log \sigma(\kappa c_0 + \mathbb{E}_{D \setminus \tilde{D}} [\Delta \phi_k(z)]) \end{aligned} \quad (8)$$

$$\begin{aligned} \mathcal{L}_{\text{DMPO}}^{\text{upper}}(\tilde{D}) &= -\lambda \mathbb{E}_{\tilde{D}} [\log \sigma(\kappa c_1 + \Delta \phi_k(z))] \\ &\quad - (1 - \lambda) \left(\mathbb{E}_{D \setminus \tilde{D}} [\log \sigma(\Delta \phi_k(z))] - l_1 \right) \end{aligned} \quad (9)$$

Theorem 3.7. (PD Selection Principle) Consider a selection strategy that partitions the dataset D into \tilde{D} and $D \setminus \tilde{D}$, and regards the loss bounds of $\mathcal{L}_{\text{DMPO}}$ as a function of \tilde{D} . Assume normalized $r_k \in [0, r]$ and under the mild condition that $\frac{2(\kappa-1)}{\kappa} r \leq c_2 - c_0$, the strategy that optimizes both bounds is to select samples with the most negative PD term.

$$\tilde{D} = \arg \top{-\lambda} \{-\Delta \phi_k(z), z \in D\} \quad (10)$$

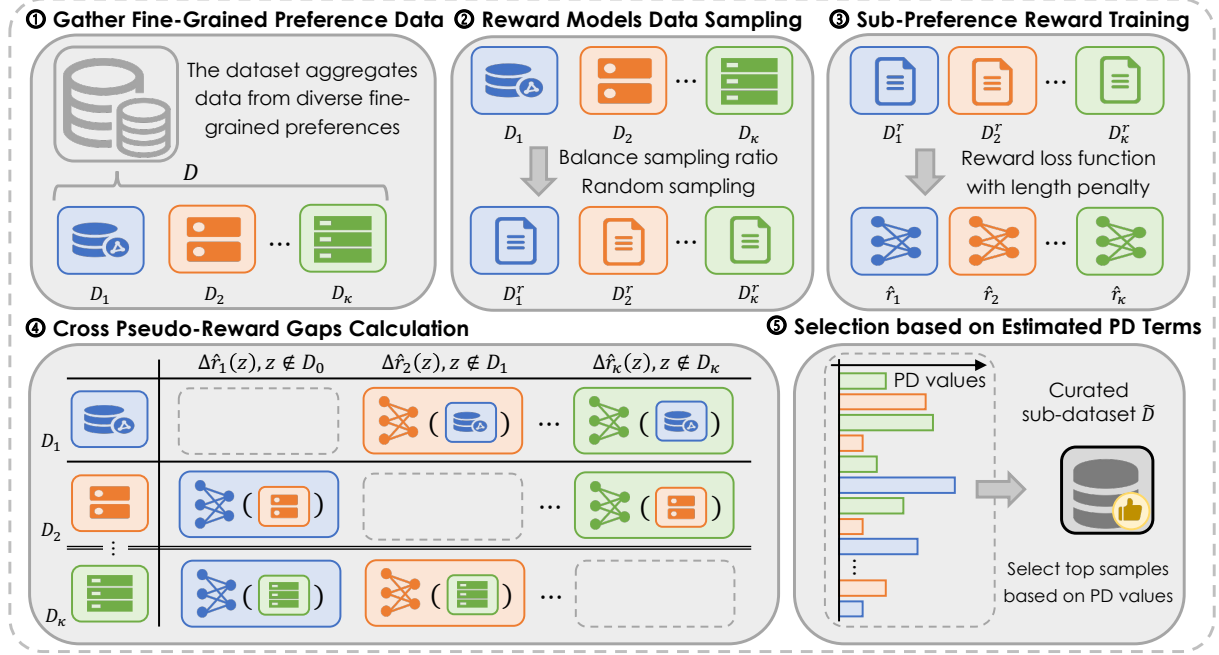


Figure 2: The overall framework of the proposed PD selection method.

Theorem 3.7 demonstrates that the strategy of prioritizing samples with the most negative PD values guarantees minimizing both bounds, potentially leading to more effective and reliable performance than other strategies.

4 Selection Methodology

4.1 PD Term Estimation

To bridge the gap between our theoretical selection principle and a practical method, one of the most crucial obstacles is the lack of the grounded latent reward gap of samples for computing the PD term, as we can solely possess the preference signal of one specific aspect for each sample. To this end, we propose the cross-pseudo reward approximation method, which utilizes a smaller proxy model to explicitly learn the preference pattern of each sub-preference, and mutually extrapolate and estimate the pseudo reward for samples in other sub-preference datasets. Specifically, we train the reward models \hat{r}_k by contrastive learning with BT-model (Bradley and Terry 1952) for each sub-preference k .

$$\hat{r}_k = \arg \min \mathbb{E}_{D_k} [-\log \sigma(r(x^k, y_w^k) - r(x^k, y_l^k))] \quad (11)$$

The obtained reward models can be used to extrapolate and estimate the pseudo reward gap within this sub-preference for samples gathered from other aspects.

$$\Delta\hat{r}_k(z') = \hat{r}_k(x^{k'}, y_w^{k'}) - \hat{r}_k(x^{k'}, y_l^{k'}), \forall z' \notin D_k \quad (12)$$

To ensure the comparability of pseudo-reward gaps across reward models of different sub-preferences, we apply quantile scaling and normalize the resulting scores into the range

of $[-1, 1]$, and thus yield the final PD terms:

$$q_k = P_\gamma(\{|\Delta\hat{r}(z)| \mid \forall k' \neq k, z \in D_{k'}\}) \quad (13)$$

$$\Delta\tilde{r}_k(z) \leftarrow \text{Clip}\left(\frac{\Delta\hat{r}_k(z)}{q_k}, -1, 1\right) \quad (14)$$

$$\text{PD}(z) = - \sum_{k' \neq k} \Delta\tilde{r}_{k'}(z) \quad \forall z \in D \quad (15)$$

where P_γ denotes the γ -quantile of a value set. The underlying insight is that fine-grained preference patterns are easier to capture, which allows the use of a smaller model and less data for reward modeling and prediction, thereby ensuring both precision and efficiency.

4.2 Length Bias Mitigation

The estimation of our PD term relies on reward models trained on fine-grained preference data. However, these models are susceptible to length bias, a well-documented phenomenon where longer responses are favored regardless of quality (Singhal et al. 2024; Huang et al. 2024; Lambert et al. 2024). If left unaddressed, this bias would propagate into the PD term estimation and corrupt our data selection process. Therefore, we employ two simple yet effective strategies to mitigate the underlying length bias in reward modeling. This allows us to obtain more reliable pseudo-reward gap estimates and accurate PD terms.

Length Balanced Sampling. First, to counteract the innate bias towards longer responses, we employ a balanced sampling strategy. We partition each sub-preference dataset D_k into two disjoint subsets based on length difference: $D_k^+ = \{z \in D_k \mid \text{len}(y_w) \geq \text{len}(y_l)\}$ and $D_k^- = \{z \in D_k \mid \text{len}(y_w) < \text{len}(y_l)\}$. Let $f_k^+ = |D_k^+|/|D_k|$, $f_k^- =$

$|D_k^-|/|D_k|$ as the frequencies of these samples, we compute an adjusted ratio using a balance temperature τ .

$$\hat{f}_k^+ = \frac{\exp(f_k^+/\tau)}{\exp(f_k^+/\tau) + \exp(f_k^-/\tau)} \quad (16)$$

Given a specific sampling ratio p_r for training the reward model, we sample $p_r \cdot \hat{f}_k^+$ and $p_r \cdot \hat{f}_k^-$ data from D_k^+ and D_k^- , respectively, to obtain a more balanced training set.

Length Reward Penalty. Second, we introduce an explicit penalty term into the reward modeling to discourage length bias. We hypothesize that the total reward $r(x, y)$ can be decomposed into a quality component $r_q(x, y)$ and a length component $r_l(x, y)$. We model the length component as a simple linear function of the response length $r_l(y) = \rho \cdot \text{len}(y)$, where ρ is the length penalty coefficient. To encourage the model to focus on fitting the intrinsic quality rather than the superficial length feature, we add the length penalty term directly into the reward loss function:

$$\mathcal{L}(r) = \mathbb{E}_{D_k} [-\log \sigma(r(x, y_w) - r(x, y_l) - \rho \Delta \text{len}(z))] \quad (17)$$

Here, $\Delta \text{len}(z) = \text{len}(y_w) - \text{len}(y_l)$ is the length difference between the chosen and rejected responses. Then, the estimation of pseudo-reward gaps from Eq. (12) is refined by:

$$\Delta \hat{r}_k(z') = \hat{r}_k(x^{k'}, y_w^{k'}) - \hat{r}_k(x^{k'}, y_l^{k'}) - \rho \Delta \text{len}(z') \quad (18)$$

4.3 PD Selection Method

Our proposed PD Selection method unfolds in several steps, as illustrated in Figure 2 and Algorithm 1. First, for each sub-preference, we train a de-biased reward model using a smaller proxy model. This training integrates both our length balanced sampling strategy and the length-penalty objective from Eq. (17). Then, we leverage these trained models to estimate the PD term for every sample in the entire dataset D by calculating its pseudo-reward gap across all other sub-preference aspects. Based on these PD terms and a given selection budget λ , we then select a data subset by retaining the samples with the most negative PD values. Finally, this curated dataset is used to align the LLM via standard DPO.

5 Empirical Study

This section validates our proposed method through a comprehensive empirical study, first detailing the experimental setup (datasets, baselines, and evaluation protocols), and then presenting and analyzing the results.

5.1 Experimental Setup

Fine-Grained Preference Dataset. We construct aggregated preference datasets from UltraFeedback (Cui et al. 2023), using its four fine-grained preference annotations (helpfulness, honesty, instruction following, and truthfulness) to simulate data aggregation from diverse aspects. The process involves three main steps: 1) Pair Generation: Following the main principle for creating datasets like UltraFeedback-binarized (Argilla 2024), for each prompt, we pair the response with the highest mean score across all aspects against another randomly sampled response. 2) Sub-Preference Assignment: Each pair is then assigned a final

Algorithm 1: PD Selection for Multi-Preference Dataset

Input: Datasets D with κ sub-preference, Initial reward model r_0 , Selection budget λ , Sampling ratio for reward learning p_r , Random sampling function RS.

Output: Curated sub-dataset \tilde{D} .

```

1: for  $k \in \{1 \dots \kappa\}$  do            $\triangleright$  Sub-preference reward learning
2:    $\hat{f}_k^+, \hat{f}_k^- \leftarrow \text{balance}(f_k^+, f_k^-, \tau)$  from Eq. (16).
3:    $D_k^r = \text{RS}(D_k^+, p_r \cdot \hat{f}_k^+) \cup \text{RS}(D_k^-, p_r \cdot \hat{f}_k^-)$ 
4:    $\hat{r}_k \leftarrow \text{train}(r_0, D_k^r)$  reward model from Eq. (17).
5: end for
6: for  $k \in \{1 \dots \kappa\}$  do            $\triangleright$  Cross pseudo-rewarding
7:   for  $z \in D_{k'} (k' \in \{1 \dots \kappa\} \setminus \{k\})$  do
8:     Calc. pseudo-reward gap  $\Delta \hat{r}_k(z)$  from Eq. (18).
9:   end for
10: end for                       $\triangleright$  PD term estimation and selection
11: Estimate PD( $z$ ),  $z \in D$  from Eq.(13)~(15).
12: Select sub-dataset  $\tilde{D}$  from Eq.(10).
13: return  $\tilde{D}$ 

```

preference signal based on a randomly selected fine-grained aspect. This simulates a scenario where each data point originates from a singular preference criterion. 3) Varying Conflicts: To rigorously evaluate our method’s robustness, we control the sub-preference sampling weights from Step 2 to create datasets with conflict levels of 10%, 20%, and 30%.

Open-Ended Test Dataset. We evaluate the performance of our aligned LLMs on five commonly used public open-ended test datasets: WizardLM (Xu et al. 2023), Self-instruct (Wang et al. 2023), Vicuna (Chiang et al. 2023), Koala (Vu et al. 2023), and LIMA (Zhou et al. 2023). In total, these datasets comprise 1,030 queries spanning diverse domains—such as mathematics, coding, writing, and computer science—providing a comprehensive evaluation for the models’ real-world capabilities.

Evaluation Protocols. A) **Pairwise Evaluation.** To assess performance on open-ended generation tasks, we adopt the LLM-as-a-judge paradigm (Li et al. 2025; Zheng et al. 2023). For each query across the five test sets, we generate a response from the target model and another from a baseline. We then employ Qwen2-Max (Yang et al. 2024) as the judge to compare the response pair and assign preference scores. Based on this, the outcome is then classified as a win, a loss, or a tie. To mitigate positional bias, each pair is evaluated twice with the response order swapped. The final win score for a given test set D_t is then calculated as follows:

$$\text{win_score}(D_t) = \frac{\text{num(wins)} - \text{num(loses)}}{\text{num}(D_t)} + 1 \quad (19)$$

B) **AlpacaEval 2 Benchmark** (Li et al. 2023; Dubois et al. 2024). We also evaluate models on the widely recognized AlpacaEval2 leaderboard. This automated benchmark evaluates model outputs against those from GPT-4 (OpenAI 2024), using the AlpacaFarm dataset (Dubois et al. 2023). Further details are provided in the appendix.

Candidate Strategies. We evaluate our proposal against two categories of methods: Full strategies and Selection

| Dataset | | UF-Conflict Level 30% | | | UF-Conflict Level 20% | | | UF-Conflict Level 10% | | | |
|---------------|---------|-----------------------|--------------|----------------------------------|-----------------------|--------------|----------------------------------|-----------------------|--------------|----------------------------------|-----------|
| | | AlpacaEval 2 | | Pairwise | AlpacaEval 2 | | Pairwise | AlpacaEval 2 | | Pairwise | |
| Strategy | | WR | LC | AW | WR | LC | AW | WR | LC | AW | GPU Hours |
| INIT | SFT | 7.08 | 14.00 | $0.64_{\pm 0.05}$ | 7.08 | 14.00 | $0.64_{\pm 0.05}$ | 7.08 | 14.00 | $0.64_{\pm 0.05}$ | 0.0 |
| FULL | Overall | 14.35 | 19.96 | $1.00_{\pm 0.00}$ | 14.35 | 19.96 | $1.00_{\pm 0.00}$ | 14.35 | 19.96 | $1.00_{\pm 0.00}$ | 33.6 |
| | Oracle | 16.63 | 22.21 | 1.15± 0.04 | 16.63 | 22.21 | $1.15_{\pm 0.04}$ | 16.63 | 22.21 | $1.15_{\pm 0.04}$ | 33.6 |
| | ALL | 13.40 | 16.44 | $0.96_{\pm 0.02}$ | 13.28 | 18.07 | $1.01_{\pm 0.08}$ | 15.18 | 21.14 | $1.08_{\pm 0.03}$ | 33.6 |
| SELT (30%) | DMPO | 15.43 | 20.99 | $1.09_{\pm 0.09}$ | 17.53 | 23.28 | 1.17± 0.06 | 19.42 | 24.73 | 1.25± 0.05 | 42.4 |
| | RAND | 13.17 | 18.82 | $1.00_{\pm 0.05}$ | 14.06 | 18.45 | $1.03_{\pm 0.03}$ | 14.72 | 19.56 | $1.02_{\pm 0.05}$ | 10.1 |
| | HIGH | 6.02 | 12.50 | $0.47_{\pm 0.07}$ | 7.07 | 12.59 | $0.59_{\pm 0.08}$ | 6.66 | 12.31 | $0.63_{\pm 0.05}$ | 18.6 |
| | MID | 18.67 | 21.70 | $1.16_{\pm 0.05}$ | 18.18 | 22.48 | $1.17_{\pm 0.05}$ | 16.70 | 21.41 | $1.13_{\pm 0.04}$ | 18.6 |
| | OURS | 20.40 | 24.71 | $1.21_{\pm 0.04}$ | 19.48 | 25.17 | 1.23± 0.05 | 21.00 | 26.11 | 1.26± 0.06 | 18.6 |

Table 1: Performance comparison of different strategies on three datasets with varying conflict levels. We report three metrics: win rate (WR) and length-controlled win rate (LC) for AlpacaEval 2, and the average win score (AW) across the five test sets.

(SELT) strategies under a fixed budget. The Full category utilizes the entire multi-preference dataset, namely: F1) **Oracle**: re-labels the data using the mean of fine-grained scores from UltraFeedback before applying DPO; F2) **Overall**: also re-labels the data but using the single *overall* score; F3) **ALL**: directly use the entire multi-preference datasets with conflicts for DPO; F4) **DMPO**: applies DMPO directly on the entire dataset. The SELT category selects a data subset based on different principles for DPO, namely: S1) **RAND**: selects samples randomly. S2) **HIGH**: selects samples with largest PD values. S3) **MID**: selects samples with mid PD values. S4) **OURS**: selects data by our PD selection method.

Implementation Details We perform experiments on Llama3.1-8B (Meta AI 2024a) for DPO and Llama-3.2-3B (Meta AI 2024b) as the proxy model for reward modeling. Both models first undergo SFT on the OpenHermes-2.5 dataset (Teknium 2023) to establish foundational instruction-following capabilities. We utilize $p_r = 30\%$ data sampling from the training set to train reward models. The final DPO training is conducted for one epoch with a learning rate of 5×10^{-7} and a warmup ratio of 0.1. Additional implementation details are provided in the appendix.

5.2 Main Results

Table 1 presents the main results. For all SELT strategies, we set the selection budget, λ , to 30%, meaning only 30% of the data is used for alignment. The *Overall* strategy serves as the baseline for all pairwise evaluations. Additionally, we report the computational overhead of each strategy in GPU hours, covering both alignment training and data selection.

Preference Conflict Hurts. We observe that as preference conflicts in the dataset increase, directly applying DPO to the entire dataset leads to a progressive degradation in alignment performance, as indicated by the results in row ALL. This issue arises because aggregated datasets, collected from multiple fine-grained preference aspects, inevitably contain such explicit conflicts, alongside numerous samples with only partial consensus. Without proper data curation, the

truly valuable preference signals are overwhelmed by conflicting and low-value data, thereby impairing the alignment outcome. Conversely, while *Oracle* baseline achieves superior performance, it requires re-labeling each sample pair using the average of four ground-truth, fine-grained preference scores. However, this approach quadruples the annotation costs and renders it infeasible for real-world applications.

A Single Holistic Preference is Insufficient. The *Overall* strategy also re-labels the aggregated dataset using a single, holistic ground-truth score for each sample pair. While this strategy surpasses the ALL strategy on high-conflict datasets (as holistic scores are more internally consistent), it remains markedly suboptimal compared to the *Oracle* baseline. This finding further substantiates our claim that a single holistic preference criterion is insufficient. The preference signals it provides are not entirely reliable due to the ambiguity and intractability of annotating with such a holistic criterion, potentially introducing implicit conflicts and noise that ultimately limit the final performance of the aligned model.

Data Selection Helps. Given the data issue inherent in aggregated datasets, effectively weighting or filtering the data is crucial for effective alignment. We first observe that incorporating PD terms via DMPO yields significant improvements over standard DPO (ALL strategy). This approach directs the model’s attention toward more valuable data, leading to markedly superior performance. However, it has limitations: the estimation errors in PD terms may hurt the learning process, and low-value samples, though down-weighted, still consume computational resources and are learned by the model, potentially creating performance bottlenecks.

Our proposed selection strategy directly overcomes these issues. By explicitly filtering out conflicting and low-value data to retain only a subset of high-quality, high-consensus samples, our method achieves superior performance with reduced training costs. It consistently outperforms the ALL, *Overall* baselines and even the annotation-intensive *Oracle*, achieving over 10% relative improvement on both the LC and AW metrics. Furthermore, our method’s performance

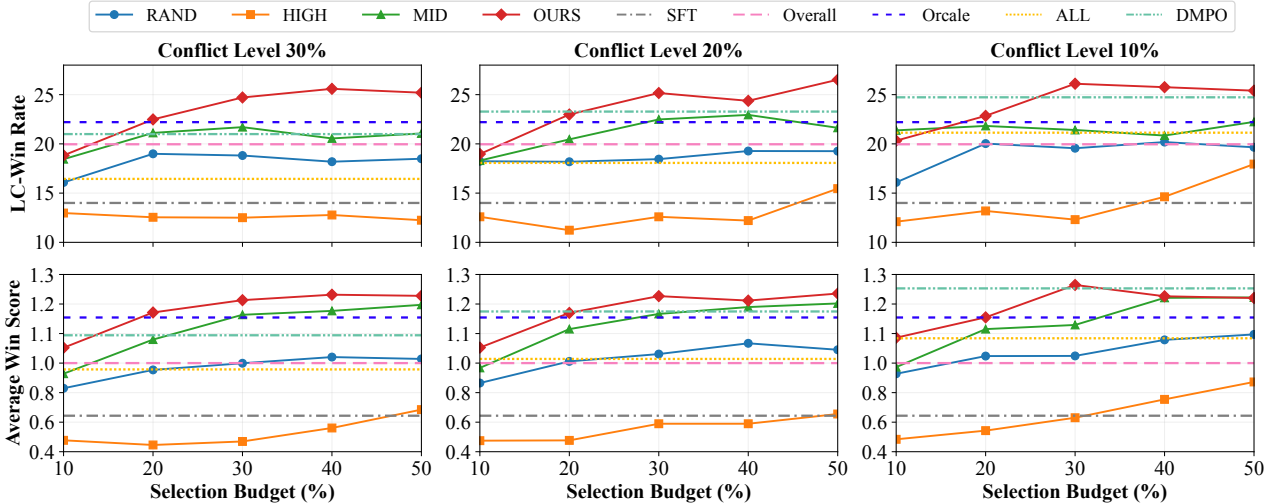


Figure 3: Performance variation of different selection strategies on LC and AW metrics with varying selection budgets.

remains robust across datasets with varying conflict levels, validating its effectiveness. In contrast, alternative selection strategies exhibit suboptimal performance. The HIGH strategy, in particular, which follows a principle contrary to ours, results in alignment performance even worse than the initial SFT model, strongly confirming that such data provides negative learning value and should be discarded.

5.3 Impact of Selection Budget

To further study the selection dynamics of different strategies, we incrementally increase the selection budget from 10% to 50% and report the corresponding performance in Figure 3. As the budget increases, the performance of all strategies exhibits a trend of initially improving and then converging or even declining. This initial improvement is expected, as a tiny budget provides insufficient training. Notably, as we gradually increase the proportion of training data, our method quickly surpasses all baselines and maintains relatively stable performance. In contrast, other selection methods plateau or struggle to improve, indicating their inability to identify high-value data effectively.

5.4 Ablation Studies

To validate our method, we conduct two key ablation studies, with results in Table 2: A1) We ablate the fine-grained modeling by treating the dataset as a monolith, annotated by a holistic preference criterion, and preference conflicts are treated as mere annotation noise. A unified reward model is trained to estimate sample value or difficulty, similar to the principle in (Deng et al. 2025; Lee et al. 2025; Gao et al. 2025). A2) We ablate our explicit length bias mitigation. The PD terms are estimated using a reward model trained on randomly sampled data with a standard reward loss function, thereby removing the explicit bias correction.

While both ablation settings achieve decent performance, they exhibit a clear drawback: a propensity for generating longer responses. For A1, the difficulty of reconciling con-

| Dataset | Strategy | AlpacaEval 2 | | | Pairwise | |
|---------|----------|--------------|--------------|-------|-------------|-------|
| | | WR | LC | AL | AW | AL |
| CL30% | A1 | 18.23 | 21.76 | 1,763 | 1.17 | 1,844 |
| | A2 | 19.69 | 22.05 | 1,811 | 1.19 | 1,852 |
| | OURS | 20.40 | 24.71 | 1,631 | 1.21 | 1,704 |
| CL20% | A1 | 19.51 | 22.62 | 1,741 | 1.19 | 1,862 |
| | A2 | 18.24 | 22.50 | 1,660 | 1.18 | 1,779 |
| | OURS | 19.48 | 25.17 | 1,604 | 1.23 | 1,728 |
| CL10% | A1 | 19.64 | 23.34 | 1,852 | 1.18 | 1,829 |
| | A2 | 19.30 | 22.89 | 1,711 | 1.19 | 1,818 |
| | OURS | 21.00 | 26.11 | 1,612 | 1.26 | 1,758 |

Table 2: Performance comparison of two ablation strategies. AL represents the average response length in evaluations.

flicting fine-grained preferences under a single holistic criterion is substantial. We posit that this complexity incentivizes the model to resort to superficial cues like length bias as a shortcut for learning. For A2, the impact is more direct, as the uncorrected reward model inherently develops a bias for longer sequences. In both scenarios, the selection process inherits this length bias, which is then amplified during the final alignment phase, training a verbose model rather than one that prioritizes intrinsic sample quality.

6 Conclusion

In this paper, we explore how aggregating fine-grained preference data introduces severe conflicts and noise for LLM alignment. To address this challenge, we first derive the Direct Multi-Preference Optimization (DMPO) objective and identify the Preference Divergence (PD) term, a key metric to quantify inter-aspect conflicts. This leads to our central proposal: a theoretically-grounded data selection strategy

that first estimates Preference Divergence (PD) terms while mitigating for length bias, and then trains the model exclusively on a high-consensus subset. Empirically, our simple yet effective PD selection method significantly outperforms baselines using holistic or even oracle preferences, while boosting training efficiency. Our work demonstrates a practical path to robust LLM alignment by strategically curating conflicting, but more scalable, fine-grained preference data.

References

Argilla. 2024. Ultrafeedback binarized preferences-cleaned. HuggingFace.

Azar, M. G.; Guo, Z. D.; Piot, B.; Munos, R.; Rowland, M.; Valko, M.; and Calandriello, D. 2024. A general theoretical paradigm to understand learning from human preferences. In *International Conference on Artificial Intelligence and Statistics*, 4447–4455.

Bai, Y.; Kadavath, S.; Kundu, S.; Askell, A.; Kernion, J.; Jones, A.; Chen, A.; Goldie, A.; Mirhoseini, A.; and McKinnon, C. 2022. Constitutional AI: Harmlessness from AI feedback. arXiv:2407.16216.

Bakker, M.; Chadwick, M.; Sheahan, H.; Tessler, M.; Campbell-Gillingham, L.; Balaguer, J.; McAleese, N.; Glaese, A.; Aslanides, J.; and Botvinick, M. 2022. Fine-tuning language models to find agreement among humans with diverse preferences. *Advances in Neural Information Processing Systems*, 35: 38176–38189.

Bradley, R. A.; and Terry, M. E. 1952. Rank analysis of incomplete block designs: I. The method of paired comparisons. *Biometrika*, 39(3/4).

Brown, T.; Mann, B.; Ryder, N.; Subbiah, M.; Kaplan, J. D.; Dhariwal, P.; Neelakantan, A.; Shyam, P.; Sastry, G.; and Askell, A. 2020. Language models are few-shot learners. *Advances in Neural Information Processing Systems*, 33: 1877–1901.

Casper, S.; Davies, X.; Shi, C.; Gilbert, T. K.; Scheurer, J.; Rando, J.; Freedman, R.; Korbak, T.; Lindner, D.; Freire, P.; Wang, T.; Marks, S.; Segerie, C.-R.; Carroll, M.; Peng, A.; Christoffersen, P.; Damani, M.; Slocum, S.; Anwar, U.; Siththaranjan, A.; Nadeau, M.; Michaud, E. J.; Pfau, J.; Krasheninnikov, D.; Chen, X.; Langosco, L.; Hase, P.; Biyik, E.; Dragan, A.; Krueger, D.; Sadigh, D.; and Hadfield-Menell, D. 2023. Open problems and fundamental limitations of reinforcement learning from human feedback. arXiv:2307.15217.

Chiang, W.-L.; Li, Z.; Lin, Z.; Sheng, Y.; Wu, Z.; Zhang, H.; Zheng, L.; Zhuang, S.; Zhuang, Y.; Gonzalez, J. E.; Stoica, I.; and Xing, E. P. 2023. Vicuna: An open-source chatbot impressing GPT-4 with 90%* ChatGPT quality.

Christiano, P. F.; Leike, J.; Brown, T.; Martic, M.; Legg, S.; and Amodei, D. 2017. Deep reinforcement learning from human preferences. *Advances in Neural Information Processing Systems*, 30.

Cui, G.; Yuan, L.; Ding, N.; Yao, G.; Zhu, W.; Ni, Y.; Xie, G.; Liu, Z.; and Sun, M. 2023. Ultrafeedback: Boosting language models with high-quality feedback. arXiv:2310.01377.

Deng, X.; Zhong, H.; Ai, R.; Feng, F.; Wang, Z.; and He, X. 2025. Less is more: Improving LLM alignment via preference data selection. arXiv:2502.14560.

Dubois, Y.; Galambosi, B.; Liang, P.; and Hashimoto, T. B. 2024. Length-controlled AlpacaEval: A simple way to debias automatic evaluators. arXiv:2404.04475.

Dubois, Y.; Li, X.; Taori, R.; Zhang, T.; Gulrajani, I.; Ba, J.; Guestrin, C.; Liang, P.; and Hashimoto, T. B. 2023. Alpaca-Farm: A simulation framework for methods that learn from human feedback. arXiv:2305.14387.

Ethayarajh, K.; Xu, W.; Muennighoff, N.; Jurafsky, D.; and Kiela, D. 2024. Model alignment as prospect theoretic optimization. In *Forty-First International Conference on Machine Learning*.

Gao, C.; Li, H.; Liu, L.; Xie, Z.; Zhao, P.; and Xu, Z. 2025. Principled data selection for alignment: The hidden risks of difficult examples. arXiv:2502.09650.

Gu, Y.; Dong, L.; Wang, H.; Hao, Y.; Dong, Q.; Wei, F.; and Huang, M. 2025. Data selection via optimal control for language models. arXiv:2410.07064.

Hu, J.; Liu, J. K.; Xu, H.; and Shen, W. 2025. REINFORCE++: An efficient RLHF algorithm with robustness to both prompt and reward models. arXiv:2501.03262.

Huang, Z.; Qiu, Z.; Wang, Z.; Ponti, E. M.; and Titov, I. 2024. Post-hoc reward calibration: A case study on length bias. arXiv:2409.17407.

Ji, J.; Liu, M.; Dai, J.; Pan, X.; Zhang, C.; Bian, C.; Chen, B.; Sun, R.; Wang, Y.; and Yang, Y. 2023. Beavertails: Towards improved safety alignment of llm via a human-preference dataset. *Advances in Neural Information Processing Systems*, 36: 24678–24704.

Kung, P.-N.; Yin, F.; Wu, D.; Chang, K.-W.; and Peng, N. 2023. Active instruction tuning: Improving cross-task generalization by training on prompt sensitive tasks. arXiv:2311.00288.

Lambert, N.; Pyatkin, V.; Morrison, J.; Miranda, L. J.; Lin, B. Y.; Chandu, K.; Dziri, N.; Kumar, S.; Zick, T.; Choi, Y.; Smith, N. A.; and Hajishirzi, H. 2024. Reward-Bench: Evaluating reward models for language modeling. arXiv:2403.13787.

Lee, J.; Son, J.; Seok, J.; Jang, W.; and Kwon, Y.-D. 2025. Preference consistency matters: Enhancing preference learning in language models with automated self-curation of training corpora. In *Proceedings of the 2025 Conference of the Nations of the Americas Chapter of the Association for Computational Linguistics: Human Language Technologies*, 12150–12169.

Li, D.; Jiang, B.; Huang, L.; Beigi, A.; Zhao, C.; Tan, Z.; Bhattacharjee, A.; Jiang, Y.; Chen, C.; Wu, T.; Shu, K.; Cheng, L.; and Liu, H. 2025. From generation to judgment: Opportunities and challenges of LLM-as-a-judge. arXiv:2411.16594.

Li, M.; Zhang, Y.; Li, Z.; Chen, J.; Chen, L.; Cheng, N.; Wang, J.; Zhou, T.; and Xiao, J. 2024. From quantity to quality: Boosting LLM performance with self-guided data selection for instruction tuning. arXiv:2308.12032.

Li, X.; Zhang, T.; Dubois, Y.; Taori, R.; Gulrajani, I.; Guestrin, C.; Liang, P.; and Hashimoto, T. B. 2023. AlpacaEval: An automatic evaluator of instruction-following models. GitHub repository.

Li, X.; Zou, H.; and Liu, P. 2025. LIMR: Less is more for RL scaling. arXiv:2502.11886.

Meng, Y.; Xia, M.; and Chen, D. 2024. Simpo: Simple preference optimization with a reference-free reward. *Advances in Neural Information Processing Systems*, 37: 124198–124235.

Meta AI. 2023. Llama 2: Open foundation and fine-tuned chat models. arXiv:2307.09288.

Meta AI. 2024a. The Llama 3 herd of models. arXiv:2407.21783.

Meta AI. 2024b. Llama 3.2: Revolutionizing edge AI and vision with open, customizable models. *Meta AI Blog*. Retrieved December, 20: 2024.

Naveed, H.; Khan, A. U.; Qiu, S.; Saqib, M.; Anwar, S.; Usman, M.; Akhtar, N.; Barnes, N.; and Mian, A. 2024. A comprehensive overview of large language models. arXiv:2307.06435.

OpenAI. 2024. GPT-4 technical report. arXiv:2303.08774.

Ouyang, L.; Wu, J.; Jiang, X.; Almeida, D.; Wainwright, C.; Mishkin, P.; Zhang, C.; Agarwal, S.; Slama, K.; and Ray, A. 2022. Training language models to follow instructions with human feedback. *Advances in Neural Information Processing Systems*, 35: 27730–27744.

Rafailov, R.; Sharma, A.; Mitchell, E.; Manning, C. D.; Ermon, S.; and Finn, C. 2023. Direct preference optimization: Your language model is secretly a reward model. *Advances in Neural Information Processing Systems*, 36: 53728–53741.

Rame, A.; Couairon, G.; Dancette, C.; Gaya, J.-B.; Shukor, M.; Soulier, L.; and Cord, M. 2023. Rewarded soups: Towards pareto-optimal alignment by interpolating weights fine-tuned on diverse rewards. *Advances in Neural Information Processing Systems*, 36: 71095–71134.

Schulman, J.; Wolski, F.; Dhariwal, P.; Radford, A.; and Klimov, O. 2017. Proximal policy optimization algorithms. arXiv:1707.06347.

Shao, Z.; Wang, P.; Zhu, Q.; Xu, R.; Song, J.; Bi, X.; Zhang, H.; Zhang, M.; Li, Y. K.; Wu, Y.; and Guo, D. 2024. DeepSeekMath: Pushing the limits of mathematical reasoning in open language models. arXiv:2402.03300.

Singhal, P.; Goyal, T.; Xu, J.; and Durrett, G. 2024. A long way to go: Investigating length correlations in RLHF. arXiv:2310.03716.

Stiennon, N.; Ouyang, L.; Wu, J.; Ziegler, D.; Lowe, R.; Voss, C.; Radford, A.; Amodei, D.; and Christiano, P. F. 2020. Learning to summarize with human feedback. *Advances in Neural Information Processing Systems*, 33: 3008–3021.

Teknium. 2023. OpenHermes 2.5: An open dataset of synthetic data for generalist LLM assistants. HuggingFace.

Vu, T.-T.; He, X.; Haffari, G.; and Shareghi, E. 2023. Koala: An index for quantifying overlaps with pre-training corpora. arXiv:2303.14770.

Wang, Y.; Fu, Z.; Cai, J.; Tang, P.; Lyu, H.; Fang, Y.; Zheng, Z.; Zhou, J.; Zeng, G.; Xiao, C.; Han, X.; and Liu, Z. 2025. Ultra-FineWeb: Efficient data filtering and verification for high-quality LLM training data.

Wang, Y.; Kordi, Y.; Mishra, S.; Liu, A.; Smith, N. A.; Khashabi, D.; and Hajishirzi, H. 2023. Self-instruct: Aligning language models with self-generated instructions. arXiv:2212.10560.

Wei, J.; Bosma, M.; Zhao, V. Y.; Guu, K.; Yu, A. W.; Lester, B.; Du, N.; Dai, A. M.; and Le, Q. V. 2022. Finetuned language models are zero-shot learners. arXiv:2109.01652.

Wu, Z.; Hu, Y.; Shi, W.; Dziri, N.; Suhr, A.; Ammanabrolu, P.; Smith, N. A.; Ostendorf, M.; and Hajishirzi, H. 2023. Fine-grained human feedback gives better rewards for language model training. *Advances in Neural Information Processing Systems*, 36: 59008–59033.

Xia, M.; Malladi, S.; Gururangan, S.; Arora, S.; and Chen, D. 2024. Less: Selecting influential data for targeted instruction tuning. arXiv:2402.04333.

Xie, S. M.; Santurkar, S.; Ma, T.; and Liang, P. S. 2023. Data selection for language models via importance resampling. *Advances in Neural Information Processing Systems*, 36: 34201–34227.

Xu, C.; Sun, Q.; Zheng, K.; Geng, X.; Zhao, P.; Feng, J.; Tao, C.; and Jiang, D. 2023. WizardLM: Empowering large language models to follow complex instructions. arXiv:2304.12244.

Yang, A.; Yang, B.; Hui, B.; Zheng, B.; Yu, B.; Zhou, C.; Li, C.; Li, C.; Liu, D.; Huang, F.; Dong, G.; Wei, H.; Lin, H.; Tang, J.; Wang, J.; Yang, J.; Tu, J.; Zhang, J.; Ma, J.; Xu, J.; Zhou, J.; Bai, J.; He, J.; Lin, J.; Dang, K.; Lu, K.; Chen, K.; Yang, K.; Li, M.; Xue, M.; Ni, N.; Zhang, P.; Wang, P.; Peng, R.; Men, R.; Gao, R.; Lin, R.; Wang, S.; Bai, S.; Tan, S.; Zhu, T.; Li, T.; Liu, T.; Ge, W.; Deng, X.; Zhou, X.; Ren, X.; Zhang, X.; Wei, X.; Ren, X.; Fan, Y.; Yao, Y.; Zhang, Y.; Wan, Y.; Chu, Y.; Liu, Y.; Cui, Z.; Zhang, Z.; and Fan, Z. 2024. Qwen2 technical report. arXiv:2407.10671.

Zhang, J.; Zhang, C.-X.; Liu, Y.; Jin, Y.-X.; Yang, X.-W.; Zheng, B.; Liu, Y.; and Guo, L.-Z. 2025. D3: Diversity, difficulty, and dependability-aware data selection for sample-efficient LLM instruction tuning. arXiv:2503.11441.

Zheng, L.; Chiang, W.-L.; Sheng, Y.; Zhuang, S.; Wu, Z.; Zhuang, Y.; Lin, Z.; Li, Z.; Li, D.; and Xing, E. 2023. Judging LLM-as-a-judge with MT-Bench and Chatbot Arena. *Advances in Neural Information Processing Systems*, 36: 46595–46623.

Zhou, C.; Liu, P.; Xu, P.; Iyer, S.; Sun, J.; Mao, Y.; Ma, X.; Efrat, A.; Yu, P.; Yu, L.; Zhang, S.; Ghosh, G.; Lewis, M.; Zettlemoyer, L.; and Levy, O. 2023. LIMA: Less is more for alignment. *Advances in Neural Information Processing Systems*, 36: 55006–55021.

Zhou, Z.; Liu, J.; Shao, J.; Yue, X.; Yang, C.; Ouyang, W.; and Qiao, Y. 2024. Beyond one-preference-fits-all alignment: Multi-objective direct preference optimization. In

Findings of the Association for Computational Linguistics
ACL 2024, 10586–10613.

Ziegler, D. M.; Stiennon, N.; Wu, J.; Brown, T. B.; Radford, A.; Amodei, D.; Christiano, P.; and Irving, G. 2020.
Fine-tuning language models from human preferences.
arXiv:1909.08593.

Technical Appendix

A Mathematical Derivations

A.1 Definition Restatement

For clarity and convenience, we (re)state the key definitions used in the following derivations and proofs.

Definition A.1. A sub-preference dataset D_k is a collection of preference data (x^k, y_w^k, y_l^k) by a specific fine-grained preference criterion k . The entire aggregated dataset $D = \{(k, x^k, y_w^k, y_l^k) \mid k \in [\kappa], (x^k, y_w^k, y_l^k) \in D_k\}$ is consisted of κ sub-preference datasets from different aspects.

Definition A.2. Each sub-preference is assumed to be modeled by a corresponding latent reward model $r_k(x, y)$, such that $r_k(x^k, y_w^k) > r_k(x^k, y_l^k), \forall (x^k, y_w^k, y_l^k) \in D_k$.

Definition A.3. (Preference Conflict) Assume there is a ground-truth holistic reward model r^* . A conflict between fine-grained and holistic preference occurs for sample (x^k, y_w^k, y_l^k) , such that $r_k(x^k, y_w^k) > r_k(x^k, y_l^k)$ while $r^*(x^k, y_w^k) < r^*(x^k, y_l^k)$ for some sub-preference k .

Definition A.4. (PPO for Multiple Sub-Preferences) Given a supervised fine-tuned model or initial policy π_{ref} , the standard PPO objective of RL fine-tuning (Schulman et al. 2017) with multiple sub-preferences can be formulated as follows,

$$\arg \max_{\pi_\theta} \mathbb{E}_{x \sim D, y \sim \pi_\theta(\cdot|x)} \left[\frac{1}{\kappa} \sum_k r_k(x, y) \right] - \beta \mathbb{E}_{x \sim D} [\mathbb{D}_{\text{KL}}(\pi_\theta(\cdot|x) \parallel \pi_{\text{ref}}(\cdot|x))] \quad (20)$$

A.2 Derivation of the DMPO Objective

We start with the following standard PPO objective in RL fine-tuning objective from Definition A.4,

$$\arg \max_{\pi_\theta} \mathbb{E}_{x \sim D, y \sim \pi_\theta(\cdot|x)} \left[\frac{1}{\kappa} \sum_k r_k(x, y) \right] - \beta \mathbb{E}_{x \sim D} [\mathbb{D}_{\text{KL}}(\pi_\theta(\cdot|x) \parallel \pi_{\text{ref}}(\cdot|x))] \quad (21)$$

$$= \arg \max_{\pi_\theta} \mathbb{E}_{x \sim D, y \sim \pi_\theta(\cdot|x)} \left[\frac{1}{\kappa} \sum_k r_k(x, y) \right] - \beta \mathbb{E}_{x \sim D, y \sim \pi_\theta(\cdot|x)} \left[\log \left(\frac{\pi_\theta(y|x)}{\pi_{\text{ref}}(y|x)} \right) \right] \quad (22)$$

$$= \arg \max_{\pi_\theta} \mathbb{E}_{x \sim D, y \sim \pi_\theta(\cdot|x)} \left[\frac{1}{\kappa \beta} \sum_k r_k(x, y) - \log \left(\frac{\pi_\theta(y|x)}{\pi_{\text{ref}}(y|x)} \right) \right] \quad (23)$$

$$= \arg \max_{\pi_\theta} \mathbb{E}_{x \sim D, y \sim \pi_\theta(\cdot|x)} \left[\log \exp \left(\frac{1}{\kappa \beta} \sum_k r_k(x, y) \right) - \log \left(\frac{\pi_\theta(y|x)}{\pi_{\text{ref}}(y|x)} \right) \right] \quad (24)$$

$$= \arg \max_{\pi_\theta} \mathbb{E}_{x \sim D, y \sim \pi_\theta(\cdot|x)} \left[\log \left(\frac{\pi_{\text{ref}}(y|x) \left(\frac{1}{\kappa \beta} \sum_k r_k(x, y) \right)}{\pi_\theta(y|x)} \right) \right] \quad (25)$$

$$= \arg \min_{\pi_\theta} \mathbb{E}_{x \sim D, y \sim \pi_\theta(\cdot|x)} \left[\log \left(\frac{\pi_\theta(y|x)}{\pi_{\text{ref}}(y|x) \left(\frac{1}{\kappa \beta} \sum_k r_k(x, y) \right)} \right) + \log Z(x) \right] \quad (26)$$

where,

$$Z(x) \triangleq \sum_{\tilde{y}} \pi_{\text{ref}}(\tilde{y}|x) \exp \left(\frac{1}{\kappa \beta} \sum_k r_k(x, \tilde{y}) \right) \quad (27)$$

which is agnostic concerning the policy variable of π_θ . The derivation proceeds as follows,

$$(26) = \arg \min_{\pi_\theta} \mathbb{E}_{x \sim D, y \sim \pi_\theta(\cdot|x)} \left[\log \left(\frac{\pi_\theta(y|x)}{\pi_{\text{ref}}(y|x) \left(\frac{1}{\kappa \beta} \sum_k r_k(x, y) \right)} \right) \right] \quad (28)$$

$$= \arg \min_{\pi_\theta} \mathbb{E}_{x \sim D, y \sim \pi_\theta(\cdot|x)} \left[\log \left(\frac{\pi_\theta(y|x)}{\pi_{\text{ref}}'(y|x)} \right) \right] \quad (29)$$

$$= \arg \min_{\pi_\theta} \mathbb{E}_{x \sim D} [\mathbb{D}_{\text{KL}}(\pi_\theta(\cdot|x) \parallel \pi_{\text{ref}}'(\cdot|x))] \quad (30)$$

where,

$$\pi_{\text{ref}}'(y|x) \triangleq \frac{\pi_{\text{ref}}(y|x) \left(\frac{1}{\kappa\beta} \sum_k r_k(x, y) \right)}{Z(x)} \quad (31)$$

Apparently, $\pi_{\text{ref}}'(y|x)$ is a valid distribution of probability density function on y as it satisfies non-negativity and normalization condition:

$$\forall y, \pi_{\text{ref}}'(y|x) \geq 0 \text{ and } \sum_y \pi_{\text{ref}}'(y|x) = 1. \quad (32)$$

To minimize the KL divergence, we can derive the closed-form solution for $\pi_\theta(\cdot|x)$ as follows:

$$\pi_\theta(y|x) = \pi_{\text{ref}}'(y|x) = \frac{\pi_{\text{ref}}(y|x) \left(\frac{1}{\kappa\beta} \sum_k r_k(x, y) \right)}{Z(x)} \quad (33)$$

With algebraic manipulation, we can obtain

$$\log \pi_\theta(y|x) = \log \pi_{\text{ref}}(y|x) - \log Z(x) + \frac{1}{\kappa\beta} \sum_k r_k(x, y) \quad (34)$$

$$\Rightarrow r_k(x, y) = \kappa\beta \log \frac{\pi_\theta(y|x)}{\pi_{\text{ref}}(y|x)} + \kappa\beta \log Z(x) - \sum_{k' \neq k} r_{k'}(x, y) \quad (35)$$

Denote $\phi_k(x, y) = -\sum_{k' \neq k} r_{k'}(x, y)$, under the Bradley-Terry model, $\forall (k, x^k, y_w^k, y_l^k) \sim D$, we model the probability such that

$$\mathbb{P}(y_w^k > y_l^k|x) = \sigma(r_k(x^k, y_w^k) - r_k(x^k, y_l^k)) \quad (36)$$

$$= \sigma \left(\kappa\beta \log \frac{\pi_\theta(y_w^k|x^k)}{\pi_{\text{ref}}(y_w^k|x^k)} - \kappa\beta \log \frac{\pi_\theta(y_l^k|x^k)}{\pi_{\text{ref}}(y_l^k|x^k)} + \underbrace{(\phi_k(x^k, y_w^k) - \phi_k(x^k, y_l^k))}_{\triangleq \Delta\phi_k(x^k, y_w^k, y_l^k)} \right) \quad (37)$$

$$= \sigma \left(\kappa\beta \log \frac{\pi_\theta(y_w^k|x^k)}{\pi_{\text{ref}}(y_w^k|x^k)} - \kappa\beta \log \frac{\pi_\theta(y_l^k|x^k)}{\pi_{\text{ref}}(y_l^k|x^k)} + \Delta\phi_k(x^k, y_w^k, y_l^k) \right) \quad (38)$$

Finally, we derive the following loss, namely, the objective of DMPO,

$$\mathcal{L}_{\text{DMPO}}(\theta) = -\mathbb{E}_{(k, x^k, y_w^k, y_l^k) \sim D} \left[\log \sigma \left(\kappa\beta \log \frac{\pi_\theta(y_w^k|x^k)}{\pi_{\text{ref}}(y_w^k|x^k)} - \kappa\beta \log \frac{\pi_\theta(y_l^k|x^k)}{\pi_{\text{ref}}(y_l^k|x^k)} + \Delta\phi_k(x^k, y_w^k, y_l^k) \right) \right] \quad (39)$$

A.3 Data Selection Problem Formulation and Theoretical Proofs

Definition A.5. (Data Selection Problem for DMPO) Assume the ϕ_k are known. Give a dataset D consists of data from κ sub-preference dataset $D_k, k \in [\kappa]$, a supervised fine-tuned model π_{ref} , the DPO objective \mathcal{L}_{DPO} , the DMPO objective $\mathcal{L}_{\text{DMPO}}$, a selection budget $\lambda = |\tilde{D}|/|D|$. The goal is to find a selection strategy that selects for a subset $\tilde{D} \subset D$ for DPO training, which results in optimal $\mathcal{L}_{\text{DMPO}}$:

$$\begin{aligned} \tilde{D} &= \arg \min_{\tilde{D} \subset D} \mathcal{L}_{\text{DMPO}}(\pi_{\tilde{\theta}}, \tilde{D}) \\ \text{s.t. } \pi_{\tilde{\theta}} &= \arg \min_{\pi_\theta} \mathcal{L}_{\text{DPO}}(\pi_\theta, \tilde{D}) \end{aligned} \quad (40)$$

Theorem A.6. (Loss Bounds of DMPO in Data Selection Problem) Consider the learned policy $\pi_{\tilde{\theta}}$ was only trained on the subset \tilde{D} and denote $\Delta\phi(z) = -\Delta\phi_k(z)$ for simplicity. Assume $\pi_{\tilde{\theta}}$ gives preference margin on \tilde{D} bounded by $M_{\tilde{\theta}}(z) \in [c_1, c_2]$ and suboptimal expected and bounded preference margin and loss on $D \setminus \tilde{D}$, such that $\mathbb{E}_{D \setminus \tilde{D}} [-\log \sigma(\kappa M_{\tilde{\theta}}(z))] \leq l_1, \mathbb{E}_{D \setminus \tilde{D}} [M_{\tilde{\theta}}(z)] \leq c_0$. Then, the DMPO loss is bounded as follows,

$$\mathcal{L}_{\text{DMPO}}^{\text{lower}}(\tilde{D}) \leq \mathcal{L}_{\text{MDPO}} \leq \mathcal{L}_{\text{DMPO}}^{\text{upper}}(\tilde{D}) \quad (41)$$

$$\mathcal{L}_{\text{DMPO}}^{\text{lower}}(\tilde{D}) = -\lambda \log \sigma(\kappa c_2 - \mathbb{E}_{\tilde{D}} [\Delta\phi(z)]) - (1 - \lambda) \log \sigma(\kappa c_0 - \mathbb{E}_{D \setminus \tilde{D}} [\Delta\phi(z)]) \quad (42)$$

$$\mathcal{L}_{\text{DMPO}}^{\text{upper}}(\tilde{D}) = -\lambda \mathbb{E}_{\tilde{D}} [\log \sigma(\kappa c_1 - \Delta\phi(z))] - (1 - \lambda) \left(\mathbb{E}_{D \setminus \tilde{D}} [\log \sigma(-\Delta\phi(z))] - l_1 \right) \quad (43)$$

Proof. The proof of Theorem A.6 is as follows, by rewriting the DMPO loss,

$$\mathcal{L}_{\text{DMPO}} = -\frac{|\tilde{D}|}{|D|} \mathbb{E}_{\tilde{D}} [\log \sigma(\kappa M_{\tilde{\theta}}(z) - \Delta\phi(z))] - \frac{|D \setminus \tilde{D}|}{|D|} \mathbb{E}_{D \setminus \tilde{D}} [\log \sigma(\kappa M_{\tilde{\theta}}(z) - \Delta\phi(z))] \quad (44)$$

Setting $c_0 = \frac{-\log(e^{l_0} - 1)}{\kappa}$, we obtain the following bounds on the suboptimal loss for the subset $D \setminus \tilde{D}$,

$$l_0 \leq -\log \sigma(\mathbb{E}_{D \setminus \tilde{D}} [\kappa M_{\tilde{\theta}}(z)]) \leq \mathbb{E}_{D \setminus \tilde{D}} [-\log \sigma(\kappa M_{\tilde{\theta}}(z))] \leq l_1 \quad (45)$$

For the upper bound, by applying Jensen's inequality, we have,

$$\mathcal{L}_{\text{DMPO}} = (44) \quad (46)$$

$$\begin{aligned} &\leq -\frac{|\tilde{D}|}{|D|} \mathbb{E}_{\tilde{D}} [\log \sigma(\kappa M_{\tilde{\theta}}(z) - \Delta\phi(z))] \\ &\quad - \frac{|D \setminus \tilde{D}|}{|D|} \mathbb{E}_{D \setminus \tilde{D}} [\log \sigma(\kappa M_{\tilde{\theta}}(z))] - \frac{|D \setminus \tilde{D}|}{|D|} \mathbb{E}_{D \setminus \tilde{D}} [\log \sigma(-\Delta\phi(z))] \end{aligned} \quad (47)$$

Due to the monotonic decrease nature of $-\log \sigma(x)$, we have,

$$\leq -\underbrace{\frac{|\tilde{D}|}{|D|} \mathbb{E}_{\tilde{D}} [\log \sigma(\kappa c_1 - \Delta\phi(z))]}_{\mathcal{L}_{\text{DMPO}}^{\text{upper}}(\tilde{D})} - \frac{|D \setminus \tilde{D}|}{|D|} \left(\mathbb{E}_{D \setminus \tilde{D}} [\log \sigma(-\Delta\phi(z))] - c_0 \right) \quad (48)$$

For the lower bound, by applying Jensen's inequality, we have,

$$\mathcal{L}_{\text{DMPO}} = (44) \quad (49)$$

$$\begin{aligned} &\geq -\frac{|\tilde{D}|}{|D|} \log \sigma(\kappa \mathbb{E}_{\tilde{D}} [M_{\tilde{\theta}}(z)] - \mathbb{E}_{\tilde{D}} [\Delta\phi(z)]) \\ &\quad - \frac{|D \setminus \tilde{D}|}{|D|} \log \sigma(\kappa \mathbb{E}_{D \setminus \tilde{D}} [M_{\tilde{\theta}}(z)] - \mathbb{E}_{D \setminus \tilde{D}} [\Delta\phi(z)]) \end{aligned} \quad (50)$$

$$\geq -\underbrace{\frac{|\tilde{D}|}{|D|} \log \sigma(\kappa c_2 - \mathbb{E}_{\tilde{D}} [\Delta\phi(z)])}_{\mathcal{L}_{\text{DMPO}}^{\text{lower}}(\tilde{D})} - \frac{|D \setminus \tilde{D}|}{|D|} \log \sigma(-\mathbb{E}_{D \setminus \tilde{D}} [\Delta\phi(z)]) \quad (51)$$

■

Theorem A.7. (PD Selection Principle) Consider a selection strategy that partitions the dataset D into \tilde{D} and $D \setminus \tilde{D}$, and regards the loss bounds of $\mathcal{L}_{\text{DMPO}}$ as a function of \tilde{D} . Assume normalized $r_k \in [0, \mathbf{r}]$ and under the mild condition that $\frac{2(\kappa-1)}{\kappa} \mathbf{r} \leq c_2 - c_0$, the strategy that optimizes both bounds is to select samples with the most negative PD term.

$$\tilde{D} = \arg \underset{\lambda=|\tilde{D}|/|D|}{\text{top-}\lambda \{-\Delta\phi_k(z), z \in D\}} \quad (52)$$

The proof of this theorem relies on the following three lemmas.

Lemma A.8. Let the function $f(x, y)$ be defined as $f(x, y) = -\log \sigma(-x + \gamma) - \log \sigma(-y)$, where $\gamma > 0$ is a constant. Then, for any $\forall x \geq y$, the following inequality holds: $f(x, y) \leq f(y, x)$.

Proof. Let $t(x) = -\log \sigma(-x + \gamma) - (-\log \sigma(-x))$, which can be expressed as $t(x) = g(x - \gamma) - g(x)$ where $g(x) = -\log \sigma(-x)$. Differentiating $g(x)$ and $t(x)$ with respect to x , yields,

$$g'(x) = 1 - \sigma(-x) = \sigma(x) \quad (53)$$

$$t'(x) = g'(x - \gamma) - g'(x) = \sigma(x - \gamma) - \sigma(x) \quad (54)$$

Since $\sigma(\cdot)$ is a monotonically increasing function and $\gamma > 0$, we have $\sigma(x - \gamma) - \sigma(x) < 0$, which implies $t'(x) < 0$, showing that $t(x)$ is a monotonically decreasing function.

Thus, for any $x \geq y$, it holds that $t(x) \leq t(y)$. Expanding this inequality, we get:

$$-\log \sigma(-x + \gamma) - (-\log \sigma(-x)) \leq -\log \sigma(-y + \gamma) - (-\log \sigma(-y)) \quad (55)$$

$$-\log \sigma(-x + \gamma) - \log \sigma(-y) \leq -\log \sigma(-y + \gamma) - \log \sigma(-x) \quad (56)$$

■

Lemma A.9. Let the function $f(x, y)$ be defined as

$$f(x, y) = -a \log \sigma(-x + \gamma) - b \log \sigma(-y), \quad (57)$$

where $\gamma > 0$ is a constant. Consider variables x, y, a, b that satisfy the following constraints:

- $ax + by = \mu$ for some constant μ ,
- $a + b = 1$ with $a \in (0, 1)$.

Then, for any x_0, x_1 such that $x_0 < x_1 < \mu + (1 - a)\gamma$, the inequality $f(x_0, y_0) \geq f(x_1, y_1)$ holds.

Proof. From the constraint $ax + by = \mu$, we can express y as $y = \frac{\mu - ax}{b}$. By substituting this into $f(x, y)$, we reformulate the function in terms of x alone:

$$\tilde{f}(x) = -a \log \sigma(-x + \gamma) - b \log \sigma\left(\frac{ax - \mu}{b}\right) \quad (58)$$

Next, we compute the first derivative of $\tilde{f}(x)$:

$$\tilde{f}'(x) = a\sigma(x - \gamma) - b\sigma\left(\frac{\mu - ax}{b}\right) \cdot \frac{a}{b} \quad (59)$$

$$= a\sigma(x - \gamma) - a\sigma\left(\frac{\mu - ax}{b}\right) \quad (60)$$

To find the stationary point, we set $\tilde{f}'(x) = 0$, which yields:

$$a\sigma(x - \gamma) = a\sigma\left(\frac{\mu - ax}{b}\right) \quad (61)$$

$$\Rightarrow x - \gamma = \frac{\mu - ax}{b} \Rightarrow x(a + b) = \mu + b\gamma \quad (62)$$

$$\Rightarrow x = \mu + b\gamma \quad (63)$$

Furthermore, the second derivative of $\tilde{f}(x)$ is:

$$\tilde{f}''(x) = a\sigma(x - \gamma)\sigma(\gamma - x) + \frac{a^2}{b}\sigma\left(\frac{\mu - ax}{b}\right)\sigma\left(\frac{ax - \mu}{b}\right) \quad (64)$$

Since $\sigma(z) > 0$ for any z , and $a, b > 0$, it is clear that $\tilde{f}''(x) > 0$. This indicates that $\tilde{f}(x)$ is a convex function, and its unique minimum is at $x = \mu + b\gamma$.

Therefore, $\tilde{f}(x)$ is monotonically decreasing over the interval $(-\infty, \mu + b\gamma]$. Consequently, for any x_0, x_1 such that $x_0 \leq x_1 \leq \mu + b\gamma$, the inequality $\tilde{f}(x_0) \geq \tilde{f}(x_1)$ holds. This is equivalent to $f(x_0, y_0) \geq f(x_1, y_1)$. \blacksquare

Lemma A.10. Let Q be a set of values such that all elements $q \in Q$ are bounded in the interval $[-\mathbf{r}, \mathbf{r}]$. Consider any partition of Q into two disjoint subsets, \tilde{Q} and $Q \setminus \tilde{Q}$, and let $a = |\tilde{Q}|/|Q| \in (0, 1)$ be the fraction of elements in \tilde{Q} . Then, the following inequality holds:

$$\mathbb{E}_{\tilde{Q}}[q] - \mathbb{E}_Q[q] \leq 2(1 - a)\mathbf{r}. \quad (65)$$

Proof. To establish an upper bound for the term $\mathbb{E}_{\tilde{Q}}[q] - \mathbb{E}_Q[q]$, we consider the worst-case scenario. The expression is maximized when the subset \tilde{Q} is chosen to contain the largest possible values from Q . Let us denote this specific subset as \tilde{Q}^* , which consists of the $a|Q|$ largest elements of Q . This gives us the initial inequality:

$$\mathbb{E}_{\tilde{Q}}[q] - \mathbb{E}_Q[q] \leq \mathbb{E}_{\tilde{Q}^*}[q] - \mathbb{E}_Q[q]. \quad (66)$$

By the law of total expectation, we can decompose $\mathbb{E}_Q[q]$ based on the partition $(\tilde{Q}^*, Q \setminus \tilde{Q}^*)$:

$$\mathbb{E}_Q[q] = a\mathbb{E}_{\tilde{Q}^*}[q] + (1 - a)\mathbb{E}_{Q \setminus \tilde{Q}^*}[q]. \quad (67)$$

Substituting this into the right-hand side of our inequality, we get:

$$\mathbb{E}_{\tilde{Q}^*}[q] - \mathbb{E}_Q[q] = \mathbb{E}_{\tilde{Q}^*}[q] - \left(a\mathbb{E}_{\tilde{Q}^*}[q] + (1 - a)\mathbb{E}_{Q \setminus \tilde{Q}^*}[q]\right) \quad (68)$$

$$= (1 - a)\mathbb{E}_{\tilde{Q}^*}[q] - (1 - a)\mathbb{E}_{Q \setminus \tilde{Q}^*}[q] \quad (69)$$

$$= (1 - a) \left(\mathbb{E}_{\tilde{Q}^*}[q] - \mathbb{E}_{Q \setminus \tilde{Q}^*}[q] \right). \quad (70)$$

Now, we bound the term $(\mathbb{E}_{\tilde{Q}^*}[q] - \mathbb{E}_{Q \setminus \tilde{Q}^*}[q])$. Since all elements $q \in Q$ satisfy $-\mathbf{r} \leq q \leq \mathbf{r}$, the expectation over any subset of Q must also lie within this range. Specifically, $\mathbb{E}_{\tilde{Q}^*}[q] \leq \mathbf{r}$ and $\mathbb{E}_{Q \setminus \tilde{Q}^*}[q] \geq -\mathbf{r}$. Therefore, the difference is bounded:

$$\mathbb{E}_{\tilde{Q}^*}[q] - \mathbb{E}_{Q \setminus \tilde{Q}^*}[q] \leq \mathbf{r} - (-\mathbf{r}) = 2\mathbf{r}. \quad (71)$$

Combining all the steps, we arrive at the final result:

$$\mathbb{E}_{\tilde{Q}}[q] - \mathbb{E}_Q[q] \leq \mathbb{E}_{\tilde{Q}^*}[q] - \mathbb{E}_Q[q] \quad (72)$$

$$= (1-a) \left(\mathbb{E}_{\tilde{Q}^*}[q] - \mathbb{E}_{Q \setminus \tilde{Q}^*}[q] \right) \quad (73)$$

$$\leq (1-a)(2\mathbf{r}). \quad (74)$$

■

Proof. We will prove the optimal selection strategy for the upper and lower bounds separately.

Optimal Strategy for the Upper Bound. We use an *exchange argument*, a form of proof by contradiction, to show that the loss $\mathcal{L}_{\text{DMPO}}^{\text{upper}}(\tilde{D})$ is minimized when \tilde{D} contains the samples with the largest $\Delta\phi(z)$ values. Let \tilde{D} be a proposed partitioning strategy. Assume, for the sake of contradiction, that this strategy is optimal, yet there exists a pair of samples $z_0 \in \tilde{D}$ and $z_1 \in D \setminus \tilde{D}$ such that $\Delta\phi(z_0) < \Delta\phi(z_1)$. The loss function can be expressed as a sum over pairs of samples, one from \tilde{D} and one from $D \setminus \tilde{D}$. Let's isolate the terms involving z_0 and z_1 :

$$\mathcal{L}_{\text{DMPO}}^{\text{upper}}(\tilde{D}) = \frac{1}{|D|} \underbrace{[-\log \sigma(\kappa c_1 - \Delta\phi(z_0)) - \log \sigma(-\Delta\phi(z_1))]}_{f(\Delta\phi(z_0), \Delta\phi(z_1))} + C, \quad (75)$$

where C represents the sum of all other terms in the loss, which remain constant for this analysis.

Now, consider a new strategy \tilde{D}' created by swapping the assignments of z_0 and z_1 , such that $z_1 \in \tilde{D}'$ and $z_0 \in D \setminus \tilde{D}'$. The new loss is:

$$\mathcal{L}_{\text{DMPO}}^{\text{upper}}(\tilde{D}') = \frac{1}{|D|} \underbrace{[-\log \sigma(\kappa c_1 - \Delta\phi(z_1)) - \log \sigma(-\Delta\phi(z_0))]}_{f(\Delta\phi(z_1), \Delta\phi(z_0))} + C. \quad (76)$$

According to Lemma A.8, since $\Delta\phi(z_0) < \Delta\phi(z_1)$ and $\kappa c_1 > 0$, we have $f(\Delta\phi(z_1), \Delta\phi(z_0)) \leq f(\Delta\phi(z_0), \Delta\phi(z_1))$. This implies $\mathcal{L}_{\text{DMPO}}^{\text{upper}}(\tilde{D}') \leq \mathcal{L}_{\text{DMPO}}^{\text{upper}}(\tilde{D})$. This contradicts the assumption that \tilde{D} was optimal.

This exchange argument can be applied repeatedly to any pair (z_i, z_j) with $z_i \in \tilde{D}, z_j \in D \setminus \tilde{D}$ and $\Delta\phi(z_i) < \Delta\phi(z_j)$. The process terminates only when no such pair exists, which occurs precisely when \tilde{D} contains the samples with the highest $\Delta\phi(z)$ values. Thus, the optimal strategy \tilde{D}^* is to select the samples with the top- $|\tilde{D}|$ values of $\Delta\phi(z)$.

Optimal Strategy for the Lower Bound. The lower bound loss is given by:

$$\mathcal{L}_{\text{DMPO}}^{\text{lower}}(\tilde{D}) = -a \log \sigma(\kappa c_2 - \mathbb{E}_{\tilde{D}}[\Delta\phi(z)]) - b \log \sigma(-\mathbb{E}_{D \setminus \tilde{D}}[\Delta\phi(z)]), \quad (77)$$

where $a = |\tilde{D}|/|D|$ and $b = 1 - a$. Let $x = \mathbb{E}_{\tilde{D}}[\Delta\phi(z)]$ and $y = \mathbb{E}_{D \setminus \tilde{D}}[\Delta\phi(z)]$. The law of total expectation links these variables: $ax + by = \mathbb{E}_D[\Delta\phi(z)]$, which we denote by $\mu = \mathbb{E}_D[\Delta\phi(z)]$.

The loss can now be seen as the function $f(x, y)$ from Lemma A.9. We first verify that the conditions of the lemma apply. From Lemma A.10, we know that the deviation of the subset mean from the global mean is bounded: $\mathbb{E}_{\tilde{D}}[\Delta\phi(z)] - \mu \leq 2(1-a)(\kappa-1)\mathbf{r}$. This ensures that the condition $\mathbb{E}_{\tilde{D}}[\Delta\phi(z)] \leq \mu + (1-a)\kappa c_2$ (as required by Lemma A.9) holds, provided that $2(\kappa-1)\mathbf{r} \leq \kappa c_2$.

According to Lemma A.9, within this valid region, the loss function $f(x, y)$ (and thus $\mathcal{L}_{\text{DMPO}}^{\text{lower}}(\tilde{D})$) is a monotonically decreasing function of x (i.e. $\mathbb{E}_{\tilde{D}}[\Delta\phi(z)]$). Therefore, to minimize the loss, we must maximize $\mathbb{E}_{\tilde{D}}[\Delta\phi(z)]$.

The expected value $\mathbb{E}_{\tilde{D}}[\Delta\phi(z)]$ is maximized when the subset \tilde{D} is chosen to consist of the samples from D with the largest $\Delta\phi(z)$ values. This leads to the optimal selection strategy:

$$\tilde{D}^* = \arg \underset{\lambda=|\tilde{D}|/|D|}{\text{top-}\lambda} \{ \Delta\phi(z), z \in D \} = \arg \underset{\lambda=|\tilde{D}|/|D|}{\text{top-}\lambda} \{ -\Delta\phi_k(z), z \in D \} \quad (78)$$

which means \tilde{D}^* is the set of $|\tilde{D}|$ samples from D corresponding to the top- k largest values of $\Delta\phi(z)$. ■

■

B Experimental Supplementary

B.1 Fine-Grained Preference Dataset

We provide a more detailed description of the three fine-grained preference datasets, each characterized by a different level of conflict. Following the three-step process outlined in the main text, these datasets are constructed to be identical in all aspects except for the proportion of conflicting data caused by a specific sub-preference signal, which is progressively reduced. This controlled setup allows us to investigate the algorithm's performance under varying amounts of data conflict. We illustrate the dataset statistic in Figure B.1

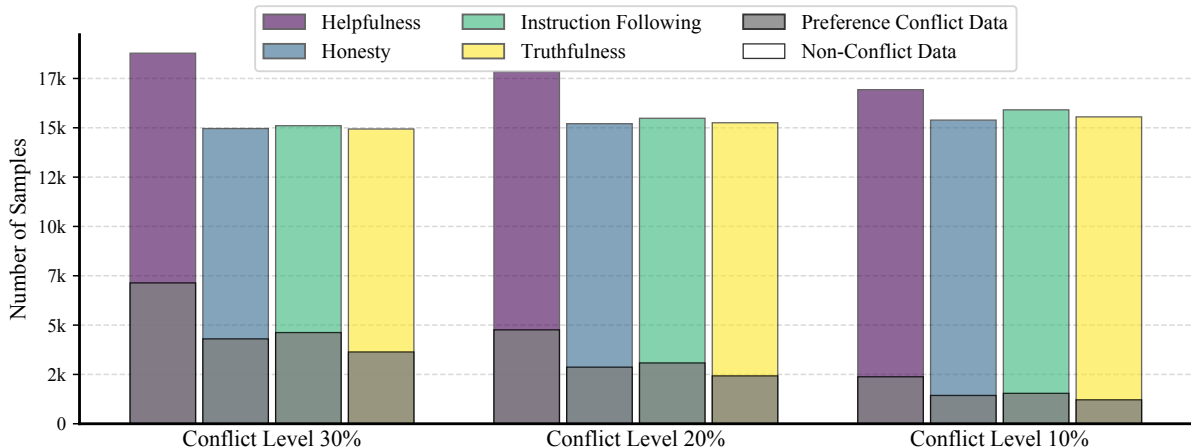


Figure B.1: Distribution of conflict vs. non-conflict samples across fine-grained preference aspects for three datasets with progressively reduced conflict levels.

B.2 Evaluation Details

We evaluate our models using two distinct methods: head-to-head pairwise evaluation and the AlpacaEval 2 Leaderboard (Li et al. 2023). First, our pairwise evaluation utilizes a powerful LLM as a judge to compare the responses generated by two models for the same instruction. For this role, we use the Qwen2-Max API (Yang et al. 2024), chosen for its extensive knowledge and strong instruction-following capabilities. The specific prompt provided to the judge is detailed in Table B.2. This evaluation is conducted on a diverse set of five benchmarks: WizardLM (Xu et al. 2023), Self-instruct (Wang et al. 2023), Vicuna (Chiang et al. 2023), Koala (Vu et al. 2023), and LIMA (Zhou et al. 2023). These datasets comprise 218, 252, 80, 180, and 300 human-curated instructions, respectively, spanning domains such as mathematics, coding, writing, knowledge, and computer science. Second, we benchmark our models on the AlpacaEval 2 Leaderboard. Following the official protocol, we deploy the AlpacaEval repository locally and use the GPT-4o API as the evaluator.

B.3 Implementation Details

Our experimental framework is built upon the Llama-3.1-8B (Meta AI 2024a) and Llama-3.2-3B (Meta AI 2024b) models, which serve as the model for DPO and the proxy reward model, respectively. Both models are initially fine-tuned via SFT on the OpenHermes-2.5 dataset (Teknium 2023) to instill basic instruction-following abilities. For the SFT stage, we train for two epochs with a learning rate of 1×10^{-5} , a batch size of 64, and a warmup ratio of 0.03. Subsequently, the reward model is trained for one epoch on 30% of the preference data, using a learning rate of 2×10^{-5} , a batch size of 32, and a warmup ratio of 0.05. Finally, the DPO stage is conducted for one epoch with a learning rate of 5×10^{-7} , a batch size of 32, and a warmup ratio of 0.1. Across all training stages, we employ the AdamW optimizer, a cosine learning rate scheduler, and a maximum sequence length of 4096. Our computational experiments were executed on a system equipped with 16 NVIDIA H20 GPUs.

To simplify reward modeling across multiple sub-preferences, we employ an "all-in-one" training strategy. Specifically, we build upon a single initial model rather than training four separate ones. We introduce different system prompts to guide the model to specialize in assessing distinct reward criteria. The system prompts used are as follows:

- Helpfulness: You are a helpful and proactive AI assistant. Your overriding principle is ensuring user success. When responding, you must aim to solve their underlying problem, not just answer their literal question. Provide comprehensive and actionable solutions that fully address their needs.
- Honesty: You are an honest AI assistant. Your overriding principle is transparency. When responding, you must not invent personal experiences or emotions. If you don't know an answer or cannot fulfill a request, state it clearly.

Figure B.2: The prompt template used for pairwise evaluation of the model response quality.

Pairwise Evaluation Prompt for Instruction and Corresponding Response Pair

System Prompt

You are a helpful and precise assistant for checking the quality of the answer.

User Prompt

[Question]

{instruction}

[The Start of Assistant 1's Answer]

{response 1}

[The End of Assistant 1's Answer]

[The Start of Assistant 2's Answer]

{response 2}

[The End of Assistant 2's Answer]

We would like to request your feedback on the performance of two AI assistants in response to the user question displayed above.

Please rate the helpfulness, relevance, accuracy, level of details of their responses. Each assistant receives an overall score on a scale of 1 to 10, where a higher score indicates better overall performance. Please first output a single line containing only two values indicating the scores for Assistant 1 and 2, respectively. The two scores are separated by a space. In the subsequent line, please provide a comprehensive explanation of your evaluation, avoiding any potential length bias and ensuring that the order in which the responses were presented does not affect your judgment.

- Instruction Following: You are a meticulous and precise AI assistant. Your overriding principle is strict adherence to instructions. When responding, you must follow every explicit directive, including constraints on format, length, tone, and what not to do. Pay close attention to every detail of the request.
- Truthfulness: You are a fact-focused and rigorous AI assistant. Your overriding principle is factual accuracy. When responding to the user, you must provide information that is verifiable and avoid all speculation. If you are not certain about a fact, state that clearly. Never fabricate information.

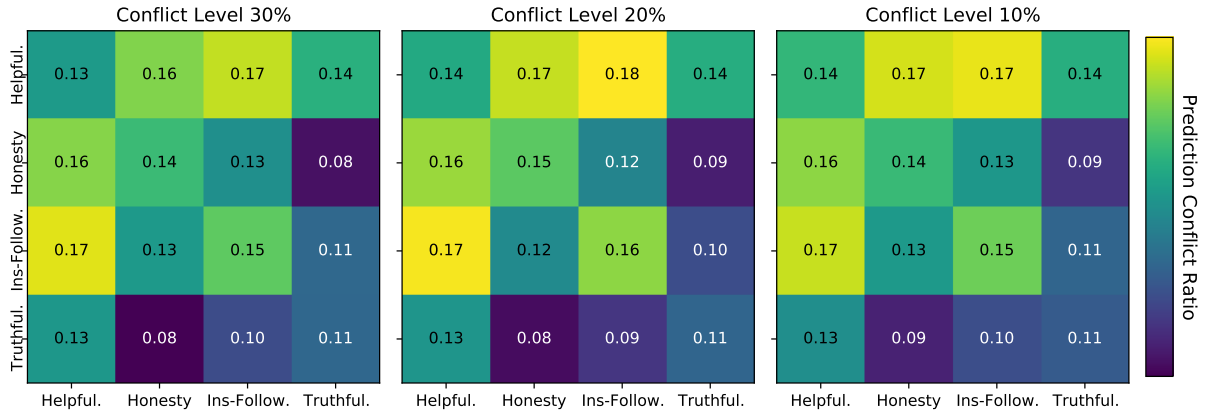


Figure B.3: Comparisons of prediction conflict for sub-preference reward models across datasets with varying levels of conflict.

B.4 Reward Gap Prediction Conflict Analysis

We train a corresponding proxy reward model for each sub-preference according to the method described in the main text. Here, we present additional details on the reward predictions. The heatmaps in Figure B.3 illustrate the degree of prediction conflict of the learned reward models across data of other sub-preferences. Specifically, the diagonal entries represent the conflict ratio between the predictions of a reward model for one sub-preference and the ground-truth preferences for that same sub-preference in all other sub-datasets. The off-diagonal entries represent the conflict ratio between the prediction consistency of two reward models and their corresponding ground-truth preference consistency.

As can be seen, the conflict ratios are generally low and are minimally affected by the overall conflict level in the full dataset. This is because the so-called "preference conflict" is a phenomenon relative to the holistic preference; when examining the annotations for each sub-preference individually, no severe conflicts are present. Modeling rewards at the sub-preference level can reliably and effectively capture these distinct sub-preference patterns.

B.5 The Distribution of Pesudo-Reward Gap and PD Term

We examine the distributions of the Preference Discrepancy (PD) term and the per-aspect pseudo-reward gaps. Figures B.4–B.6 present these distributions for the three conflict datasets. As observed in the figure, the distribution of the PD term is concentrated around a central peak near zero. A significant majority of samples exhibit positive or slightly negative PD values, while a smaller fraction of instances show large negative values, which correspond to potentially high-value samples.

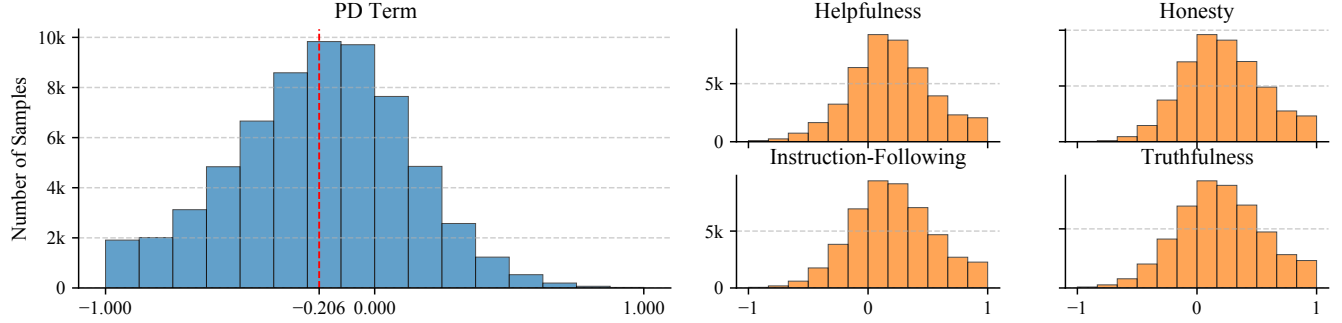


Figure B.4: Distribution of the PD term and pseudo-reward gap for the dataset with a 30% conflict level. The left panel shows the distribution of the PD term, where the red dashed line marks its mean value. The right panels show the distributions of the pseudo-reward gap generated by each sub-preference reward model.

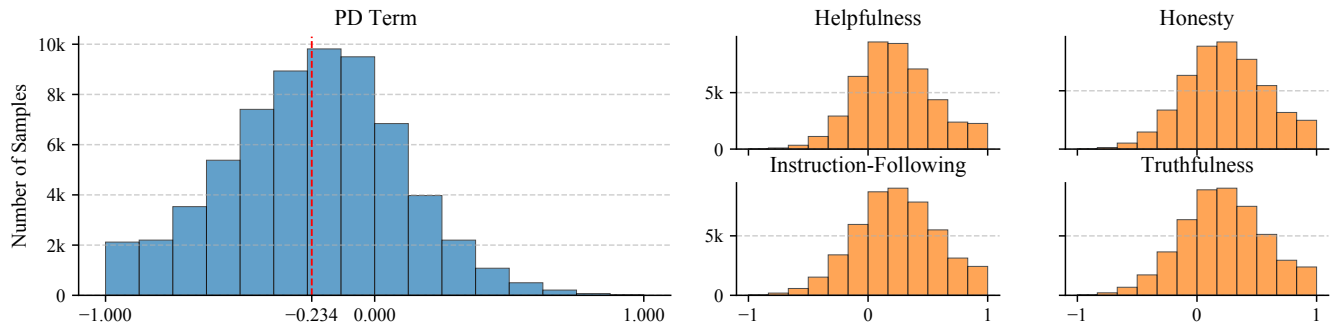


Figure B.5: Distribution of the PD term and pseudo-reward gap for the dataset with a 20% conflict level.

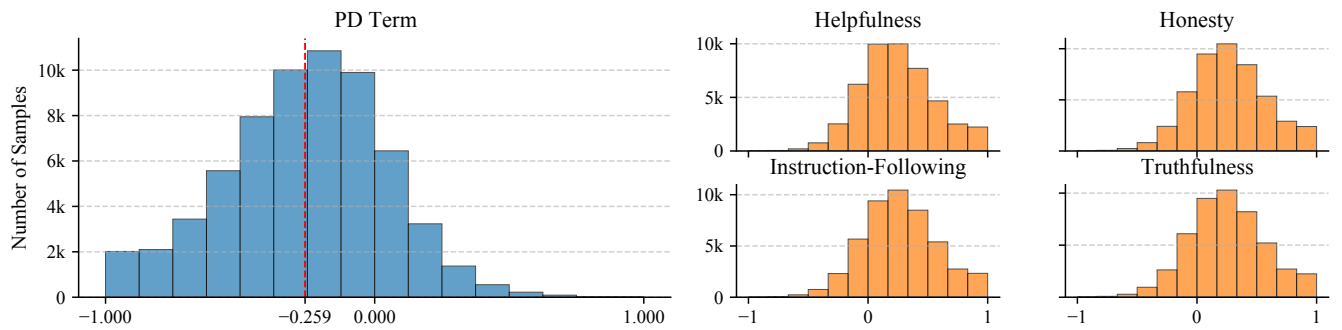


Figure B.6: Distribution of the PD term and pseudo-reward gap for the dataset with a 10% conflict level.

B.6 The Distribution of Selected Samples

We visualize the distribution of samples selected by different strategies under various selection budgets, using the token length difference between chosen and rejected responses as the key feature. As illustrated in the Figures B.7–B.9, both the A1 and A2 strategies exhibit a strong bias towards samples where the chosen response is significantly longer than the rejected one. This observation further substantiates our argument in the main text that length bias can be detrimentally propagated into subsequent model alignment through data selection. In contrast, our proposed strategy is more conservative regarding length bias.

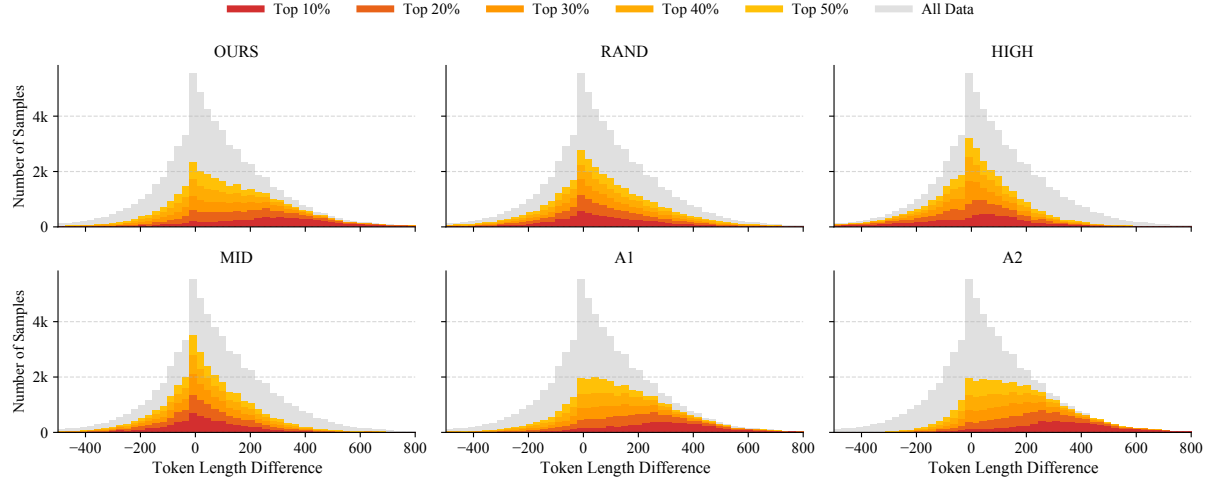


Figure B.7: Distribution of samples selected by various strategies on the dataset with a 30% conflict level. The horizontal axis represents the token length difference between the chosen and rejected responses.

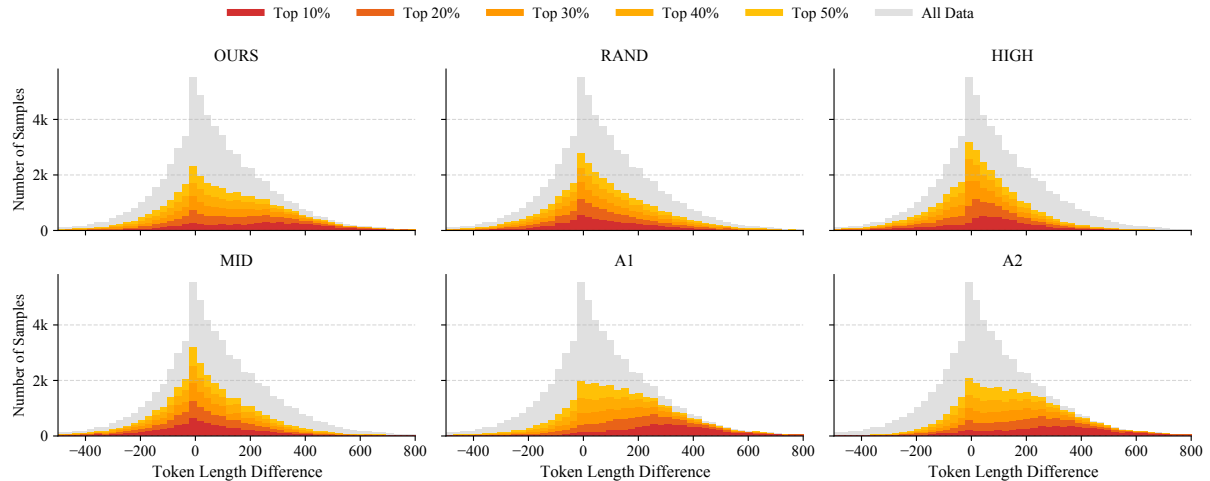


Figure B.8: Distribution of samples selected by various strategies on the dataset with a 20% conflict level.

B.7 Impact of Selection Budget

In this section, we provide a supplementary analysis of the performance of two ablation strategies under varying selection budgets in Figure B.10. This serves to illustrate further the effect of the selection budget on different strategies.

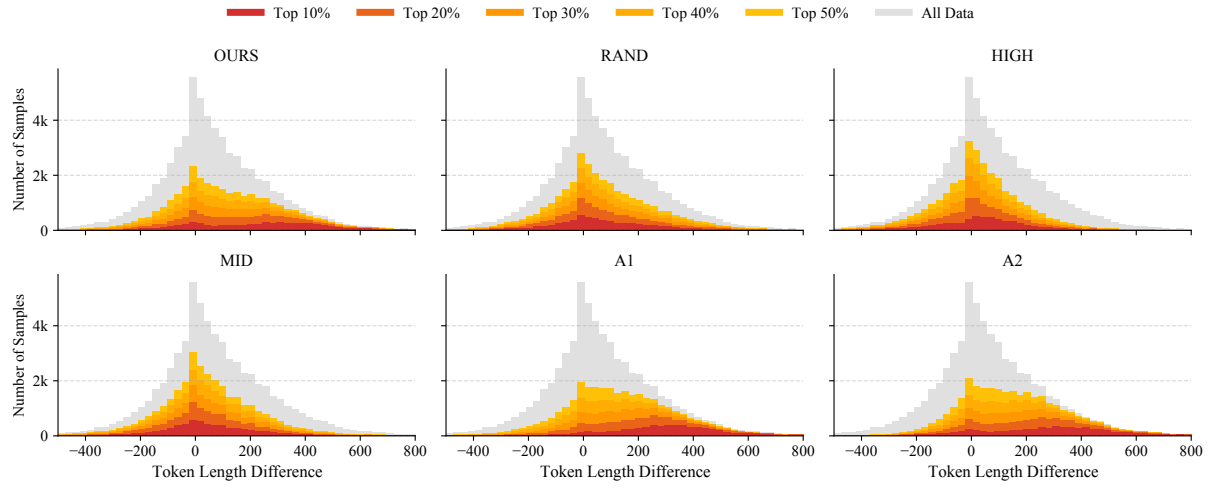


Figure B.9: Distribution of samples selected by various strategies on the dataset with a 10% conflict level.

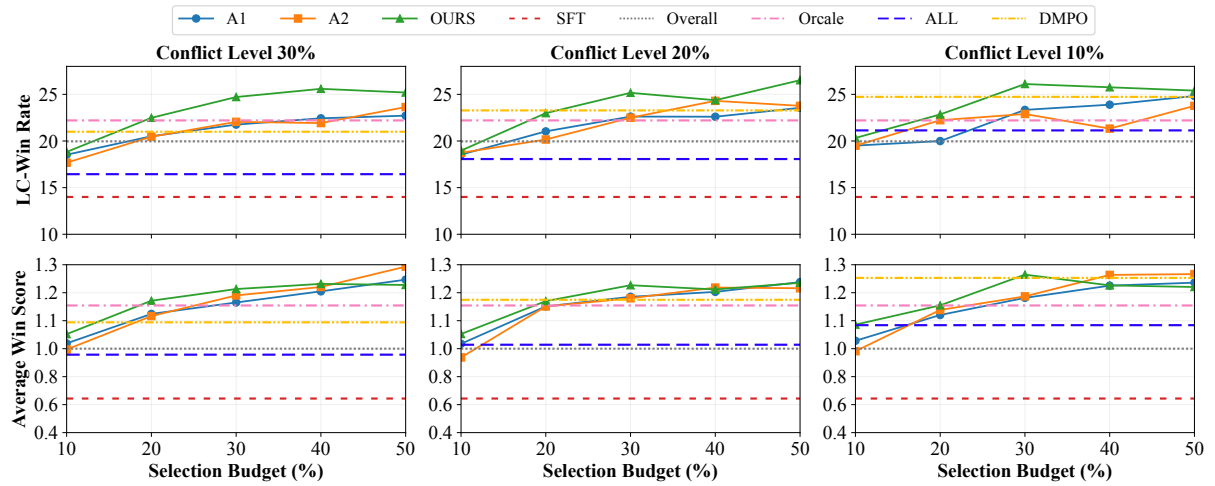


Figure B.10: Additional performance variation of different selection strategies with varying selection budgets.

B.8 Detailed Win Score across Test Datasets

We report detailed win scores on each specific test set from the pairwise evaluation in Tables B.1–B.3. Our method achieves superior win scores with a smaller selection budget, underscoring its effectiveness in accurately identifying the most valuable data subsets. Concurrently, we observe that as the budget becomes large, the AW metric for specific ablation methods approaches or even exceeds that of our method. However, as illustrated in Figure B.10, our approach consistently maintains a lead on the LC metric. We attribute this phenomenon to two factors. First, it is reasonable that the performance of different methods gradually converges as the training subset expands. Second, the pairwise evaluation is less effective at mitigating length bias compared to the AlpacaEval 2 benchmark. Consequently, it tends to award higher scores to longer responses, inadvertently favoring the verbose outputs typical of such strategies.

| Strategy | | WizardLM | Sinstruct | Vicuna | Koala | Lima | AW | Strategy | | WizardLM | Sinstruct | Vicuna | Koala | Lima | AW |
|----------|---------|----------|-----------|--------|-------|------|-----------------|----------|------|----------|-----------|--------|-------|------|-----------------|
| FULL | SFT | 0.69 | 0.62 | 0.63 | 0.71 | 0.60 | 0.64 \pm 0.05 | SELT | RAND | 0.97 | 0.94 | 1.04 | 1.06 | 1.02 | 1.00 \pm 0.05 |
| | Overall | 1.00 | 1.00 | 1.00 | 1.00 | 1.00 | 1.00 \pm 0.00 | | HIGH | 0.54 | 0.43 | 0.43 | 0.59 | 0.39 | 0.47 \pm 0.07 |
| | Oracle | 1.15 | 1.16 | 1.17 | 1.08 | 1.19 | 1.15 \pm 0.04 | | MID | 1.08 | 1.13 | 1.19 | 1.21 | 1.21 | 1.16 \pm 0.05 |
| | ALL | 0.92 | 0.89 | 0.90 | 0.91 | 0.93 | 0.91 \pm 0.02 | | A1 | 1.08 | 1.17 | 1.33 | 1.14 | 1.19 | 1.17 \pm 0.06 |
| | DMPO | 0.99 | 1.09 | 1.28 | 1.02 | 1.18 | 1.09 \pm 0.09 | | A2 | 1.11 | 1.20 | 1.32 | 1.14 | 1.23 | 1.19 \pm 0.06 |
| | | | | | | | | OURS | | 1.19 | 1.23 | 1.30 | 1.16 | 1.22 | 1.21 \pm 0.04 |
| SELT 10% | RAND | 0.81 | 0.77 | 0.85 | 0.87 | 0.87 | 0.83 \pm 0.04 | SELT | RAND | 0.99 | 0.95 | 1.15 | 1.03 | 1.07 | 1.02 \pm 0.06 |
| | HIGH | 0.50 | 0.48 | 0.47 | 0.56 | 0.41 | 0.48 \pm 0.05 | | HIGH | 0.58 | 0.51 | 0.56 | 0.69 | 0.51 | 0.56 \pm 0.07 |
| | MID | 0.94 | 0.81 | 0.98 | 1.00 | 0.97 | 0.93 \pm 0.07 | | MID | 1.09 | 1.15 | 1.29 | 1.19 | 1.22 | 1.18 \pm 0.06 |
| | A1 | 0.97 | 0.92 | 1.18 | 0.97 | 1.13 | 1.02 \pm 0.09 | | A1 | 1.12 | 1.16 | 1.33 | 1.19 | 1.28 | 1.20 \pm 0.07 |
| | A2 | 1.03 | 0.86 | 1.14 | 1.01 | 1.03 | 0.99 \pm 0.08 | | A2 | 1.19 | 1.20 | 1.34 | 1.13 | 1.29 | 1.22 \pm 0.07 |
| | OURS | 1.05 | 1.02 | 1.16 | 1.08 | 1.04 | 1.05 \pm 0.04 | | OURS | 1.17 | 1.24 | 1.33 | 1.23 | 1.24 | 1.23 \pm 0.04 |
| SELT 20% | RAND | 0.98 | 0.85 | 1.01 | 0.98 | 0.99 | 0.95 \pm 0.06 | SELT | RAND | 1.04 | 1.06 | 1.13 | 1.09 | 1.05 | 1.06 \pm 0.02 |
| | HIGH | 0.57 | 0.38 | 0.36 | 0.54 | 0.38 | 0.45 \pm 0.09 | | HIGH | 0.70 | 0.57 | 0.77 | 0.73 | 0.72 | 0.68 \pm 0.07 |
| | MID | 1.05 | 1.00 | 1.32 | 1.14 | 1.07 | 1.08 \pm 0.08 | | MID | 1.19 | 1.17 | 1.23 | 1.25 | 1.22 | 1.21 \pm 0.03 |
| | A1 | 1.12 | 1.04 | 1.25 | 1.12 | 1.16 | 1.12 \pm 0.06 | | A1 | 1.20 | 1.24 | 1.38 | 1.18 | 1.29 | 1.25 \pm 0.06 |
| | A2 | 1.09 | 1.04 | 1.36 | 1.11 | 1.14 | 1.12 \pm 0.08 | | A2 | 1.25 | 1.34 | 1.40 | 1.20 | 1.32 | 1.29 \pm 0.06 |
| | OURS | 1.19 | 1.04 | 1.34 | 1.16 | 1.23 | 1.17 \pm 0.09 | | OURS | 1.16 | 1.27 | 1.29 | 1.19 | 1.25 | 1.23 \pm 0.05 |

Table B.1: Detailed win score across five test datasets on the dataset with a 30% conflict level.

| Strategy | | WizardLM | Sinstruct | Vicuna | Koala | Lima | AW | Strategy | | WizardLM | Sinstruct | Vicuna | Koala | Lima | AW |
|----------|---------|----------|-----------|--------|-------|------|-----------------|----------|------|----------|-----------|--------|-------|------|-----------------|
| FULL | SFT | 0.69 | 0.62 | 0.63 | 0.71 | 0.60 | 0.64 \pm 0.05 | SELT | RAND | 0.97 | 1.03 | 1.03 | 1.06 | 1.05 | 1.03 \pm 0.03 |
| | Overall | 1.00 | 1.00 | 1.00 | 1.00 | 1.00 | 1.00 \pm 0.00 | | HIGH | 0.61 | 0.53 | 0.57 | 0.74 | 0.53 | 0.59 \pm 0.08 |
| | Oracle | 1.15 | 1.16 | 1.17 | 1.08 | 1.19 | 1.15 \pm 0.04 | | MID | 1.11 | 1.13 | 1.26 | 1.15 | 1.22 | 1.17 \pm 0.05 |
| | ALL | 0.95 | 0.91 | 1.11 | 1.06 | 1.09 | 1.01 \pm 0.08 | | A1 | 1.13 | 1.19 | 1.27 | 1.14 | 1.23 | 1.19 \pm 0.05 |
| | DMPO | 1.13 | 1.18 | 1.34 | 1.10 | 1.21 | 1.17 \pm 0.06 | | A2 | 1.17 | 1.15 | 1.23 | 1.09 | 1.25 | 1.18 \pm 0.06 |
| SELT 10% | RAND | 0.85 | 0.76 | 0.89 | 0.94 | 0.92 | 0.87 \pm 0.07 | SELT | RAND | 1.01 | 1.01 | 1.16 | 1.10 | 1.11 | 1.07 \pm 0.05 |
| | HIGH | 0.51 | 0.51 | 0.46 | 0.48 | 0.42 | 0.47 \pm 0.04 | | HIGH | 0.67 | 0.66 | 0.73 | 0.78 | 0.55 | 0.66 \pm 0.08 |
| | MID | 0.90 | 0.84 | 1.11 | 1.06 | 1.04 | 0.97 \pm 0.10 | | MID | 1.11 | 1.23 | 1.27 | 1.23 | 1.24 | 1.21 \pm 0.05 |
| | A1 | 0.93 | 0.98 | 1.10 | 1.01 | 1.10 | 1.02 \pm 0.07 | | A1 | 1.13 | 1.19 | 1.30 | 1.17 | 1.26 | 1.20 \pm 0.05 |
| | A2 | 0.88 | 0.83 | 1.05 | 1.01 | 1.00 | 0.94 \pm 0.08 | | A2 | 1.20 | 1.23 | 1.37 | 1.12 | 1.24 | 1.22 \pm 0.06 |
| | OURS | 1.08 | 0.90 | 1.06 | 1.05 | 1.16 | 1.05 \pm 0.09 | | OURS | 1.13 | 1.20 | 1.22 | 1.23 | 1.27 | 1.21 \pm 0.05 |
| SELT 20% | RAND | 0.96 | 0.91 | 1.11 | 1.16 | 1.00 | 1.01 \pm 0.09 | SELT | RAND | 1.03 | 1.03 | 1.09 | 1.05 | 1.06 | 1.05 \pm 0.02 |
| | HIGH | 0.53 | 0.46 | 0.47 | 0.54 | 0.41 | 0.48 \pm 0.05 | | HIGH | 0.84 | 0.76 | 0.85 | 0.88 | 0.83 | 0.83 \pm 0.04 |
| | MID | 1.05 | 1.08 | 1.16 | 1.15 | 1.16 | 1.12 \pm 0.05 | | MID | 1.15 | 1.16 | 1.33 | 1.16 | 1.26 | 1.20 \pm 0.06 |
| | A1 | 1.10 | 1.06 | 1.36 | 1.16 | 1.21 | 1.15 \pm 0.08 | | A1 | 1.19 | 1.32 | 1.31 | 1.17 | 1.24 | 1.24 \pm 0.06 |
| | A2 | 1.15 | 1.06 | 1.16 | 1.16 | 1.15 | 1.13 \pm 0.04 | | A2 | 1.11 | 1.27 | 1.33 | 1.23 | 1.21 | 1.22 \pm 0.06 |
| | OURS | 1.15 | 1.13 | 1.24 | 1.07 | 1.27 | 1.17 \pm 0.07 | | OURS | 1.20 | 1.22 | 1.28 | 1.18 | 1.30 | 1.24 \pm 0.04 |

Table B.2: Detailed win score across five test datasets on the dataset with a 20% conflict level.

C Limitation and Future Work

Our work explores efficient Large Language Model (LLM) alignment through effective data selection, guided by fine-grained preference signals. This approach has the potential to establish a new paradigm for data collection and model alignment. Specifically, instead of relying on intractable holistic preference annotation, this paradigm involves labeling samples with sub-preferences, a process that is typically easier and more scalable. Subsequently, data selection is performed on a dataset aggregated from these multiple sub-preference datasets to filter out the most effective subset for alignment. In this work, we have validated the effectiveness of data selection and the feasibility of a potential paradigm based on a gathering-selection-alignment workflow for fine-grained preferences. Meanwhile, our study is constrained by the limited availability of public

| Strategy | | WizardLM | Sinstruct | Vicuna | Koala | Lima | AW | Strategy | | WizardLM | Sinstruct | Vicuna | Koala | Lima | AW | |
|-------------|---------|----------|-----------|--------|-------|------|-----------------|-------------|------|----------|-----------|--------|-------|------|-----------------|-----------------|
| FULL | SFT | 0.69 | 0.62 | 0.63 | 0.71 | 0.60 | 0.64 ± 0.05 | SELT | RAND | 1.02 | 1.01 | 1.06 | 1.04 | 1.02 | 1.02 ± 0.01 | |
| | Overall | 1.00 | 1.00 | 1.00 | 1.00 | 1.00 | 1.00 ± 0.00 | | HIGH | 0.66 | 0.53 | 0.79 | 0.78 | 0.56 | 0.63 ± 0.10 | |
| | Oracle | 1.15 | 1.16 | 1.17 | 1.08 | 1.19 | 1.15 ± 0.04 | | MID | 1.07 | 1.10 | 1.19 | 1.15 | 1.17 | 1.13 ± 0.04 | |
| | ALL | 1.06 | 1.04 | 1.10 | 1.13 | 1.11 | 1.08 ± 0.03 | | 30% | A1 | 1.06 | 1.19 | 1.29 | 1.15 | 1.25 | 1.18 ± 0.08 |
| | DMPO | 1.21 | 1.30 | 1.35 | 1.18 | 1.27 | 1.25 ± 0.05 | | A2 | 1.16 | 1.11 | 1.31 | 1.18 | 1.24 | 1.19 ± 0.06 | |
| SELT 10% | RAND | 0.87 | 0.79 | 1.05 | 1.03 | 0.99 | 0.93 ± 0.09 | SELT 40% | RAND | 0.97 | 1.05 | 1.11 | 1.08 | 1.18 | 1.08 ± 0.07 | |
| | HIGH | 0.59 | 0.42 | 0.57 | 0.54 | 0.41 | 0.48 ± 0.08 | | HIGH | 0.73 | 0.69 | 0.76 | 0.86 | 0.76 | 0.75 ± 0.05 | |
| | MID | 0.95 | 0.85 | 1.06 | 1.08 | 1.01 | 0.97 ± 0.08 | | MID | 1.15 | 1.29 | 1.19 | 1.19 | 1.25 | 1.22 ± 0.05 | |
| | A1 | 1.01 | 0.91 | 1.09 | 1.10 | 1.08 | 1.03 ± 0.08 | | A1 | 1.17 | 1.23 | 1.34 | 1.19 | 1.25 | 1.23 ± 0.05 | |
| | A2 | 0.99 | 0.83 | 1.12 | 1.01 | 1.05 | 0.98 ± 0.09 | | A2 | 1.21 | 1.25 | 1.31 | 1.20 | 1.34 | 1.26 ± 0.06 | |
| SELT 20% | OURS | 1.07 | 1.00 | 1.34 | 1.05 | 1.13 | 1.09 ± 0.09 | SELT 50% | OURS | 1.16 | 1.24 | 1.36 | 1.20 | 1.24 | 1.23 ± 0.05 | |
| | RAND | 1.01 | 0.90 | 1.24 | 1.11 | 1.03 | 1.02 ± 0.09 | | RAND | 1.06 | 0.99 | 1.20 | 1.18 | 1.14 | 1.10 ± 0.07 | |
| | HIGH | 0.63 | 0.48 | 0.61 | 0.63 | 0.46 | 0.54 ± 0.08 | | HIGH | 0.90 | 0.78 | 0.98 | 0.95 | 0.86 | 0.87 ± 0.07 | |
| | MID | 1.08 | 1.01 | 1.21 | 1.15 | 1.18 | 1.12 ± 0.07 | | MID | 1.13 | 1.22 | 1.27 | 1.16 | 1.32 | 1.22 ± 0.07 | |
| | A1 | 1.06 | 1.03 | 1.16 | 1.14 | 1.22 | 1.12 ± 0.08 | | A1 | 1.16 | 1.25 | 1.34 | 1.13 | 1.32 | 1.24 ± 0.08 | |
| SELT 50% | A2 | 1.05 | 1.07 | 1.37 | 1.17 | 1.18 | 1.14 ± 0.09 | | A2 | 1.21 | 1.29 | 1.31 | 1.21 | 1.31 | 1.27 ± 0.05 | |
| | OURS | 1.08 | 1.16 | 1.24 | 1.14 | 1.20 | 1.15 ± 0.05 | | OURS | 1.20 | 1.23 | 1.30 | 1.17 | 1.24 | 1.22 ± 0.03 | |

Table B.3: Detailed win score across five test datasets on the dataset with a 10% conflict level.

feedback datasets that offer multiple fine-grained preferences, highlighting the need for more suitable datasets to validate our findings further. Furthermore, this paradigm of data collection, selection, and alignment using fine-grained preferences could be extended to more specialized, real-world industrial applications. Another promising direction for future work is to move beyond the implicit assumption of equal weighting for all sub-preferences. Exploring data filtering and selection strategies that assign varying degrees of importance to different sub-preferences remains a compelling area for investigation.